

1-1-2019

## Cationic biaryl 1,2,3-triazolyl peptidomimetic amphiphiles: synthesis, antibacterial evaluation and preliminary mechanism of action studies

Andrew J. Tague

Papanin Putsathit  
*Edith Cowan University*

Katherine A. Hammer

Steven M. Wales

Daniel R. Knight

*See next page for additional authors*

Follow this and additional works at: <https://ro.ecu.edu.au/ecuworkspost2013>

 Part of the [Microbiology Commons](#)

---

[10.1016/j.ejmech.2019.02.013](https://doi.org/10.1016/j.ejmech.2019.02.013)

© 2019. This manuscript version is made Available under the CC-BY-NC-ND 4.0 license  
<http://creativecommons.org/licenses/by-nc-nd/4.0/>

This is an Author's Accepted Manuscript of: Tague, A. J., Putsathit, P., Hammer, K. A., Wales, S. M., Knight, D. R., Riley, T. V., . . . Pyne, S. G. (2019). Cationic biaryl 1,2,3-triazolyl peptidomimetic amphiphiles: Synthesis, antibacterial evaluation and preliminary mechanism of action studies. *European Journal of Medicinal Chemistry*, 386-404.

Available [here](#)

This Journal Article is posted at Research Online.

<https://ro.ecu.edu.au/ecuworkspost2013/5950>

---

**Authors**

Andrew J. Tague, Papanin Putsathit, Katherine A. Hammer, Steven M. Wales, Daniel R. Knight, Thomas V. Riley, Paul A. Keller, and Stephen G. Pyne

© 2019. This manuscript version is made available under the CC-BY-NC-ND 4.0 license  
<http://creativecommons.org/licenses/by-nc-nd/4.0/>



# Cationic biaryl 1,2,3-triazolyl peptidomimetic amphiphiles targeting *Clostridioides (Clostridium) difficile*: synthesis, antibacterial evaluation and an *in vivo* *C. difficile* infection model

Andrew J. Tague<sup>a†</sup>, Papanin Putsathit<sup>b</sup>, Melanie L. Hutton<sup>c</sup>, Katherine A. Hammer<sup>d</sup>, Steven M. Wales<sup>a</sup>, Daniel R. Knight<sup>e</sup>, Thomas V. Riley<sup>b,d,e,f</sup>, Dena Lyras<sup>c</sup>, Paul A. Keller<sup>a†</sup> and Stephen G. Pyne<sup>a†</sup>

<sup>a</sup>School of Chemistry and Molecular Bioscience, University of Wollongong, Wollongong, NSW 2522, Australia

<sup>b</sup>School of Medical and Health Sciences, Edith Cowan University, Western Australia 6027, Australia

<sup>c</sup>Infection and Immunity Program, Monash Biomedicine Discovery Institute and Department of Microbiology, Monash University, Clayton, VIC, 3800, Australia

<sup>d</sup>School of Biomedical Sciences, The University of Western Australia, Western Australia 6009, Australia

<sup>e</sup>School of Veterinary and Life Sciences, Murdoch University, Western Australia 6150, Australia

<sup>f</sup>PathWest Laboratory Medicine, Queen Elizabeth II Medical Centre, Western Australia 6009, Australia

† Corresponding authors: [atague@uow.edu.au](mailto:atague@uow.edu.au) (A. Tague)  
[keller@uow.edu.au](mailto:keller@uow.edu.au) (P. Keller)  
[spyne@uow.edu.au](mailto:spyne@uow.edu.au) (S. Pyne)

## Abstract

*Clostridioides* (formerly *Clostridium*) *difficile* is a Gram-positive anaerobic bacterial pathogen that causes severe gastrointestinal infection in humans. The current chemotherapeutic options are vastly inadequate, expensive and limited; this results in an exorbitant medical and financial burden. New, inexpensive chemotherapeutic treatments for *C. difficile* infection with improved efficacy are urgently needed. A streamlined synthetic pathway was developed to allow access to 38 novel mono- and di-cationic biaryl 1,2,3-triazolyl peptidomimetics with increased synthetic efficiency, aqueous solubility and enhanced antibacterial efficacy. The monocationic arginine derivative **28** was identified as a potent, Gram-positive selective antibacterial with MIC values of 4 µg/mL against methicillin-resistant *Staphylococcus aureus* and 8 µg/mL against *C. difficile*. Furthermore, the dicationic bis-triazole analogue **50** was found to exhibit broad-spectrum activity with substantial Gram-negative efficacy against *Acinetobacter baumannii* (8 µg/mL), *Pseudomonas aeruginosa* (8 µg/mL) and *Klebsiella pneumoniae* (16 µg/mL); additionally, compound **50** displayed reduced haemolytic activity (<13%) in an *in vitro* haemolysis assay. Membrane-disruption assays were conducted on selected derivatives to confirm the membrane-active mechanism of action inherent to the synthesized amphiphilic compounds. A comparative solubility assay was developed and utilized to optimize the aqueous solubility of the compounds for *in vivo* studies. The biaryl peptidomimetics **28** and **67** were found to exhibit significant efficacy in an *in vivo* murine model of *C. difficile* infection by reducing the severity and slowing the onset of disease.

## Keywords:

Antibacterial

*Clostridioides (Clostridium) difficile*

Peptidomimetic

Biaryl cationic amphiphiles

Triazole

## 1. Introduction

*Clostridioides* (formerly *Clostridium*) *difficile* is a Gram-positive, anaerobic bacterium that causes mild to serious infections in the gastrointestinal (GI) tract due to the potent toxins and resilient endospores that are produced by the organism [1-2]. *C. difficile* infection (CDI) occurs when the normal GI microbiota is compromised by conventional antibiotics; this allows *C. difficile* to flourish in the GI tract due to the absence of the usual enteric microbiome [1-2]. Broad spectrum antibiotic therapy indiscriminately destroys the GI microflora, but fails to eradicate *C. difficile* spores [3]; this unwanted side-effect allows *C. difficile* to infect up to 20% of hospital patients administered oral antibiotics [1]. *C. difficile* produces robust endospores that are resistant to most antibiotics, alcohol-based hand sanitizers, heat and freezing [3]. The hospital setting provides a prime ‘breeding

ground' for *C. difficile* spores, which can stay viable for months at a time [1-2]. Almost all broad-spectrum antibiotics can instigate CDI by eliminating the commensal GI microflora; however, antibiotics such as ampicillin/amoxicillin, cephalosporins, clindamycin and fluoroquinolones are most commonly associated with CDI [1].

CDI exhibits an overall mortality rate of up to 8% [2] and infection recurrence occurs in up to 20% of cases treated with first-line chemotherapeutics (i.e. vancomycin or metronidazole) [4]. Both the severity and incidence of CDI cases has increased in the last decade due to epidemics of hypervirulent *C. difficile* strains, e.g. PCR ribotype 027 – also known as strain B1/NAP1/027 [1-2]. This ribotype exhibits a mortality rate that is three times higher than normal *C. difficile* isolates [1]. The prevalence of *C. difficile* infection results in a massive financial burden on the modern healthcare system (≤\$4.8 billion per annum) [5]. The CDC issued a report in 2013 entitled 'Antibiotic Resistance Threats'; *C. difficile* was listed as the number one bacterial threat facing the healthcare sector and humans in general.<sup>[6]</sup> A recent update by the CDC reports that CDI is responsible for approximately 500,000 infections and 15,000 deaths annually in the USA – the highest of any of the bacterial threats listed by the CDC [5]. Due to the high levels of infection, recurrence, mortality, cost and the lack of adequate treatments for CDI, there exists a substantial incentive to pursue novel chemotherapeutics that effectively combat CDI.

Antibacterial selectivity for *C. difficile* is an essential component for a fully effective CDI chemotherapeutic. The elimination of all GI bacteria by broad-spectrum antibacterial activity provides an ideal habitat for *C. difficile* spores to grow; therefore, the maintenance and/or restoration of commensal GI microflora is essential for preventing CDI recurrence [1-3]. Fecal transplantation has thus become a viable method for treating cases of chronic/severe CDI, as it physically replaces the commensal GI microflora [1-2, 7]. The classic chemotherapeutic treatments for CDI (i.e. vancomycin and metronidazole) suffer from efficacy issues, most notably CDI recurrence, due to their lack of selectivity for *C. difficile* and inability to prevent sporulation [1-2].

Fidaxomicin was approved by the FDA in 2011 and it is the only new small-molecule chemotherapeutic that has been specifically approved for use against CDI [8]; it exhibits approximately 50% less CDI recurrence relative to vancomycin [9]. Furthermore, the increased efficacy of fidaxomicin is thought to be a result of its selectivity for *C. difficile* over commensal enteric microflora (i.e. *Bacteroides* spp.) and its ability to reduce *C. difficile* sporulation [3, 10]. There are numerous potential chemotherapeutics undergoing clinical trials for use in the treatment of CDI; examples include CRS3123 (National Institute for Allergy and Infectious Disease) [4, 11-12], LFF571 (Novartis) [13-16], NVB302 (Novacta Biosystems) [4, 3, 17], ridinilazole (Summit Pharmaceuticals) [18-19] and cadazolid (Actelion Ltd.) [20-22]. Many other small molecule chemotherapeutics are currently under investigation for use in the battle against *C. difficile*, such as various synthetic derivatives of purines [23], macrolides [24], nitroheterocycles [25], glycopeptides [26], tetramic acids [27], antimicrobial peptidomimetics [28-29], nylon-3 polymers [30] and bis-indoles [31]. Immunotherapeutic approaches include vaccination and passive antibody therapy; so far, these therapies have all focused on the *C. difficile* toxins. There are two vaccines currently being independently investigated in clinical trials by Pfizer and Intercell [3]. In October 2016, bezlotoxumab (Merck's monoclonal antibody targeting *C. difficile* toxin B) was given FDA approval as an adjunct therapy for patients who are currently undergoing antibiotic therapy for CDI treatment and are at high risk of recurrent infection [32]. There exists a drastic need for more efficacious chemotherapeutics for the treatment of CDI; a well-tolerated and safe medication that could selectively target *C. difficile* (and its spores), while leaving the enteric microbiome intact, would prove invaluable in the treatment of severe and recurrent CDI.

Recent work in our laboratory has generated a class of cationic amphiphilic biarylpeptidomimetics (e.g. lead compound **1**, Fig. 1) that have been shown to exert antibacterial activity through cytoplasmic membrane disruption [28].

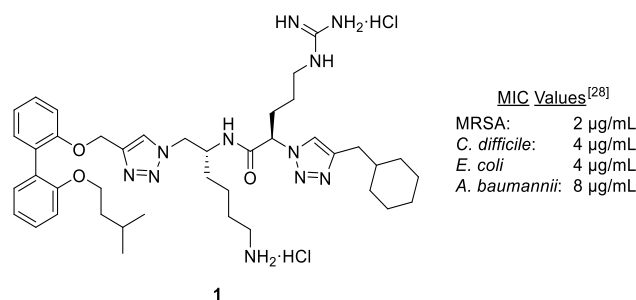


**Fig. 1.** Lead peptidomimetic compound **1**.

These membrane-active peptidomimetic derivatives exhibit potent broad-spectrum activity against Gram-positive and Gram-negative pathogenic bacteria (Fig. 1) [28-29]. Previous reports have shown that the major pharmacophore components required for antimicrobial activity are a biaryl aromatic core with attached cationic residues and hydrophobic residues [29, 28, 33-35]. This pharmacophore model parallels other antimicrobial peptide mimic models, like those proposed by Haldar *et al.* [36] and Kumar *et al.* [37]. The mixture of cationic and hydrophobic residues attached to the scaffold backbone confers an amphiphilic conformation to the molecules, which is essential for membrane disruption and antibacterial activity. Prior work has furnished multiple 1,2,3-triazole containing amphiphilic peptidomimetics with strong activity against *C. difficile* (MIC = 4 µg/mL) [28-29]; these biarylpeptidomimetics were investigated as potential CDI treatments due to their potential low oral bioavailability and promising *in vitro* activity against *C. difficile* [29].

Utilizing lead compound **1** as a starting point and the established pharmacophore as a guide, three new series of amphiphiles were developed to allow for facile synthetic access to novel biaryl 1,2,3-triazole peptidomimetics for investigation as potential CDI chemotherapeutics. A simplified synthetic pathway was designed and utilized to obtain 38 final antibiotic derivatives which were subjected to *in vitro* antibacterial activity testing against a range of Gram-positive and Gram-negative pathogenic bacteria. Membrane disruption (i.e. cytoplasmic membrane depolarization and permeabilization) assays were performed on prototypical derivatives to confirm their mode of action. *In vitro* haemolysis and cytotoxicity assays were also performed on specific derivatives. A comparative solubility assay was designed and utilized to investigate the relative aqueous solubility of the peptidomimetics for *in vivo* administration. Selected peptidomimetics from this study and previous studies [29, 28] were then subjected to a murine *in vivo* *C. difficile* infection model to ascertain their viability as chemotherapeutic agents for the treatment of CDI. Preliminary pharmacokinetics analysis of the mouse blood and feces was conducted to verify a lack of systemic absorption.

## 2. Results and Discussion

### 2.1 Design, synthesis and characterization of cationic biaryl peptidomimetic amphiphiles

Three series of cationic biaryl 1,2,3-triazolyl amphiphiles were designed and synthesized for antibacterial evaluation as potential *C. difficile* chemotherapeutics: monocationic amide analogues (**A**), dicationic amide analogues (**B**) and dicationic bis-triazole derivatives (**C**) (Fig. 2).

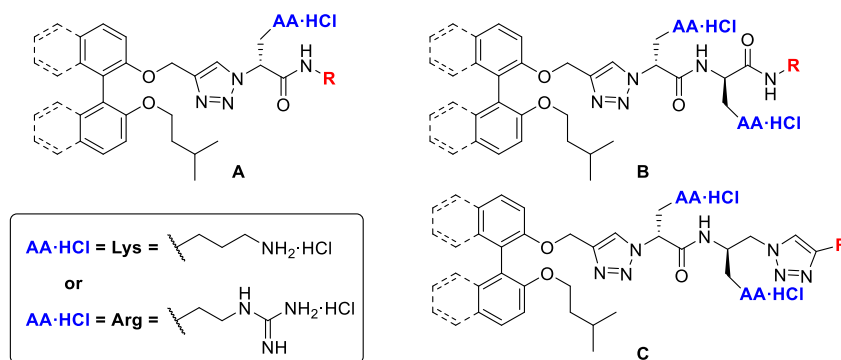


**Fig. 2.** General structures of the cationic biaryl 1,2,3-triazolyl peptidomimetic amphiphiles (Series **A**, **B** and **C**).

In an attempt to streamline synthetic access to the amphiphilic derivatives, a modified backbone structure was developed based upon lead compound **1**, previous studies [29, 33-35, 38-39] and the known pharmacophore requirements. It was envisioned that a reversed peptide orientation (Fig. 3) would allow for a shorter synthetic pathway without compromising antibacterial efficacy.

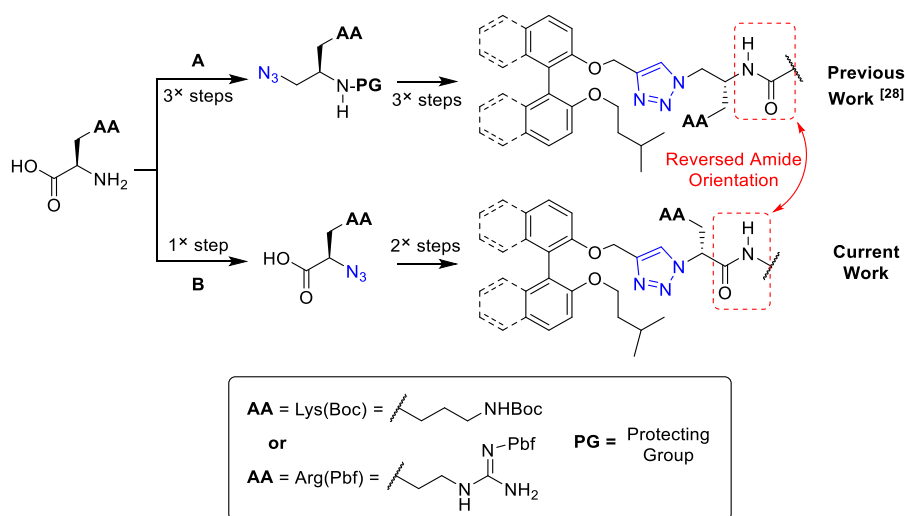
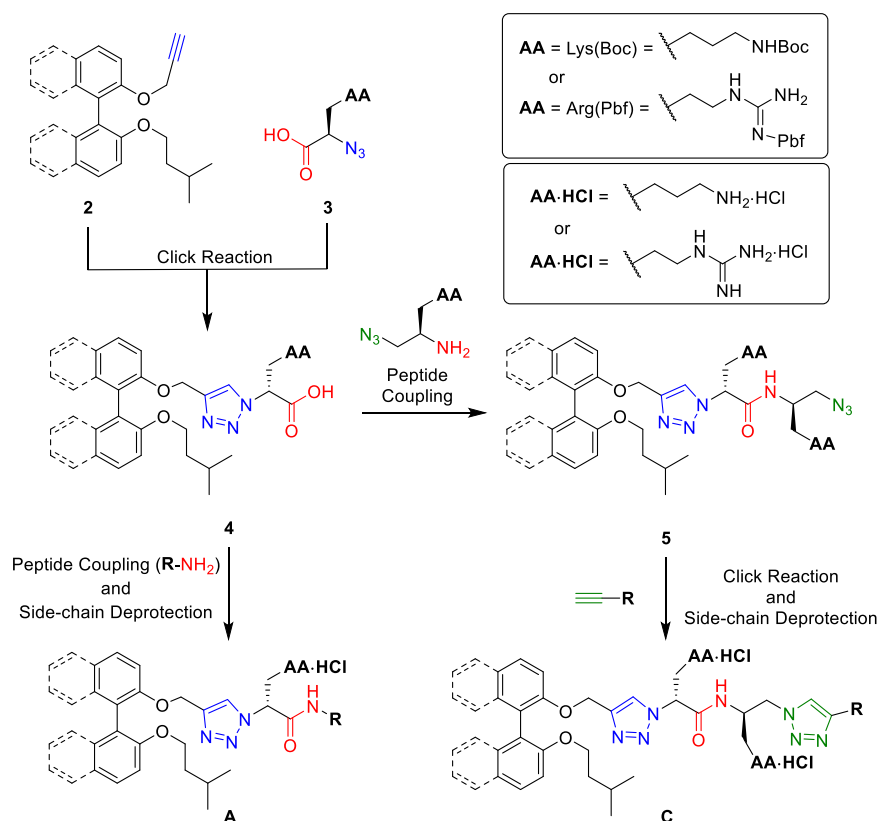


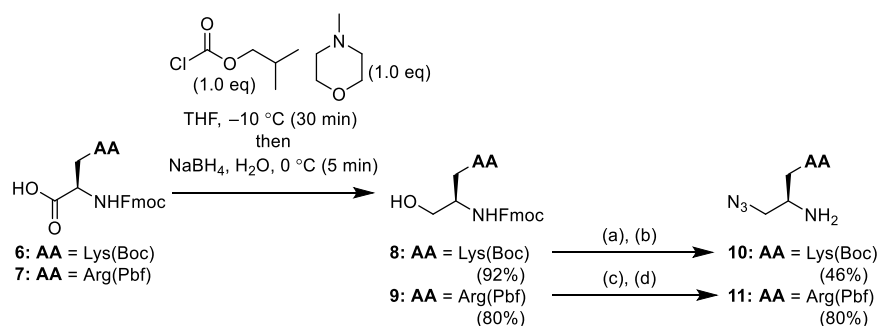
**Fig. 3.** Comparison of the previous synthetic pathway **A** (6× steps) [28] and current synthetic pathway **B** (3× steps); note the variation in the resultant peptide backbone orientation.

In order to furnish a library with enhanced structural diversity, variation of the biaryl core (i.e. (*S*)-binaphthyl or biphenyl), cationic amino acid residues (i.e. Lys and/or Arg) and the hydrophobic termini linker (i.e. amide or 1,2,3-triazole) were undertaken to obtain the different amphiphilic derivatives of Series **A**, **B** and **C**. Unnatural *D*-configured amino acids were utilized for enhanced metabolic stability against proteases in the mammalian GI tract [40]. An overview of the modular synthetic pathway is exemplified in Scheme 1; a small pool of key precursor building blocks were combined *via* copper-catalysed azide-alkyne cycloaddition (CuAAC) and peptide coupling reactions to furnish the desired scaffolds (e.g. compounds **4** and **5**). These scaffolds served as divergence points in the synthetic pathway; multiple antimicrobial peptidomimetics were thus obtained through facile derivatization of the corresponding scaffolds *via* CuAAC or peptide coupling reactions followed by acidolytic side-chain *N*-deprotection and subsequent hydrochloride salt formation (Scheme 1).



**Scheme 1.** Example of the modular synthetic pathway utilized to achieve Series **A** and Series **C** derivatives.

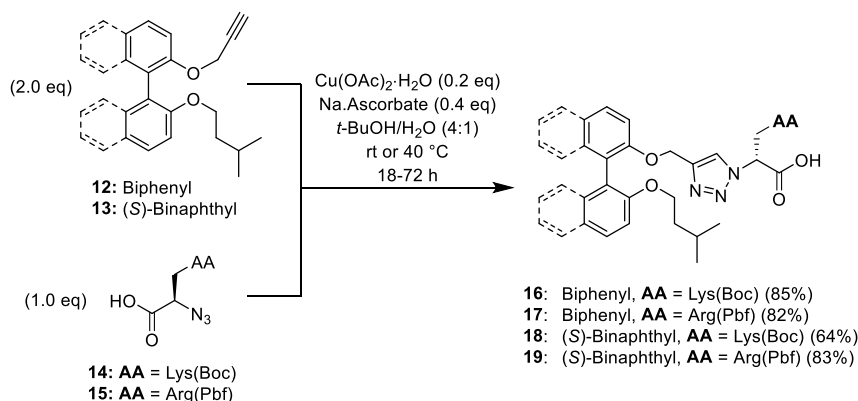
The required azido amine fragments were synthesized from commercially available *N*-Fmoc-*D*-amino acids. The *N*-Fmoc amino acids (**6** and **7**) were reduced to their corresponding alcohols (**8** and **9**) [41] *via* mixed anhydride reduction with  $\text{NaBH}_4$  [42] (Scheme 2). Initially, azido amine **10** [29] was realized by mesylation of alcohol **8** followed by azidation in DMF (Scheme 2); unfortunately, the amine was obtained in lower yields due to competing oxazolidinone formation during the azidation step. To avoid this issue during the synthesis of azido amine **11**, the reported procedure [29] was followed with slight modification; the iodide intermediate was subjected to  $\text{S}_{\text{N}}2$  displacement with  $\text{NaN}_3$  at 20 °C before raising the temperature to 50 °C to promote *N*-Fmoc deprotection [43], thus preventing the possibility of oxazolidinone formation (Scheme S1). Chromatographic purification of the amine product was eliminated in favour of an acid/base isolation procedure.



**Scheme 2.** Synthesis of azido amines **10** and **11**. **Reagents and conditions:** (a)  $\text{CH}_3\text{SO}_2\text{Cl}$  (1.5 eq),  $\text{NEt}_3$  (1.5 eq),  $\text{CH}_2\text{Cl}_2$ , 0 °C (15 min)  $\rightarrow$  rt (1 h); (b)  $\text{NaN}_3$  (5.0 eq), DMF, 50 °C (18 h); (c)  $\text{I}_2$  (1.1 eq),  $\text{PPh}_3$  (1.1 eq), imidazole (1.2 eq),  $\text{CH}_2\text{Cl}_2$ , rt (20 h); (d)  $\text{NaN}_3$  (5.0 eq), DMF, 20 °C (4 h)  $\rightarrow$  50 °C (18 h).

With the required precursors in hand, the Series **A** scaffold acids (**16–19**) were then constructed by CuAAC reaction between an (*S*)-binaphthyl or biphenyl alkyne core (**12** or **13**) [28] and an azido acid component (**14** or **15**) [28] (Scheme 3). Analysis of the gHMBC NMR spectrum of scaffold derivative **28** allowed for unequivocal proof of the 1,4-regioselectivity (Fig. S3).





**Scheme 3.** Synthesis of Series A scaffold acids **16–19** by CuAAC reaction.

When the  $^{13}\text{C}$  NMR spectra of the scaffold acids **16–19** were acquired in  $\text{CDCl}_3$  or  $\text{CD}_3\text{OD}$ , the triazole carbons and the adjacent methine and carboxyl carbons (Fig. 4) could not be assigned to a corresponding resonance; the use of 2-D NMR (i.e. gHMBC and/or gHSQC) and/or  $\text{DMSO-}d_6$  was necessary to properly assign the carbon resonances. Furthermore, the  $^1\text{H}$  NMR resonances assigned to the methine and triazole protons were often extremely broad or completely unobservable without 2-D NMR analysis. Inter- or intra-molecular hydrogen bonding between the carboxylic acid functionality and the internal triazole moiety was the likely cause behind this NMR phenomena, as the anomalies were not observed amongst the amide derivatives of the scaffold acids.

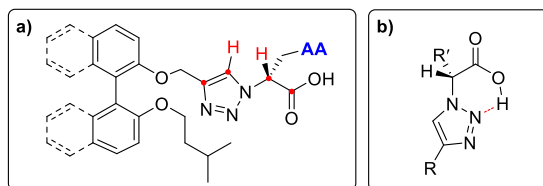
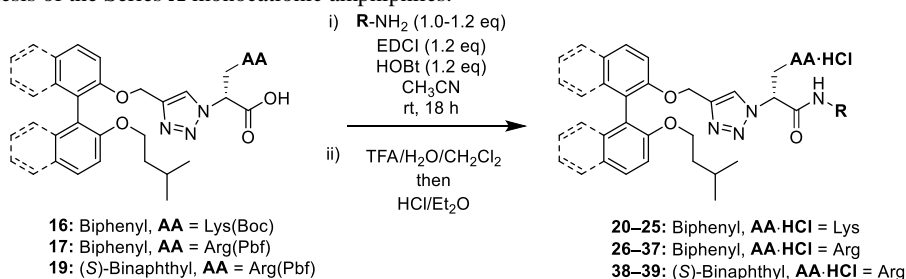


**Fig. 4.** a) General structure of scaffold acids that exhibited weak or non-observable NMR resonances; the affected carbons and protons are marked with red ( $\bullet$  or H); b) Potential intramolecular hydrogen bonding (----) between the 1,2,3-triazole and the adjacent carboxylic acid moiety.

Derivatization of the Series A scaffold acids (**16–19**) was thus accomplished by peptide bond formation with various hydrophobic amines ( $\text{R-NH}_2$ ) and EDCI/HOBt in  $\text{CH}_3\text{CN}$ ; subsequent *N*-deprotection of the cationic side-chains with TFA/ $\text{CH}_2\text{Cl}_2/\text{H}_2\text{O}$  followed by treatment with ethereal HCl yielded the Series A monocationic amphiphiles **20–39** (Table 1) as their hydrochloride salts.

**Table 1.** Synthesis of the Series A monocationic amphiphiles.



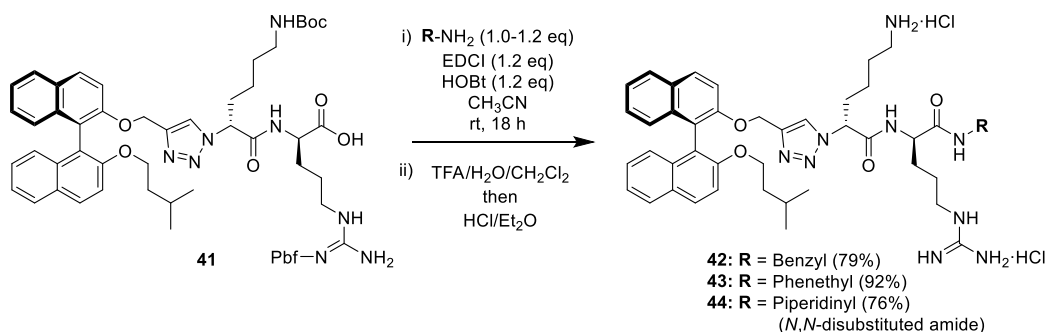
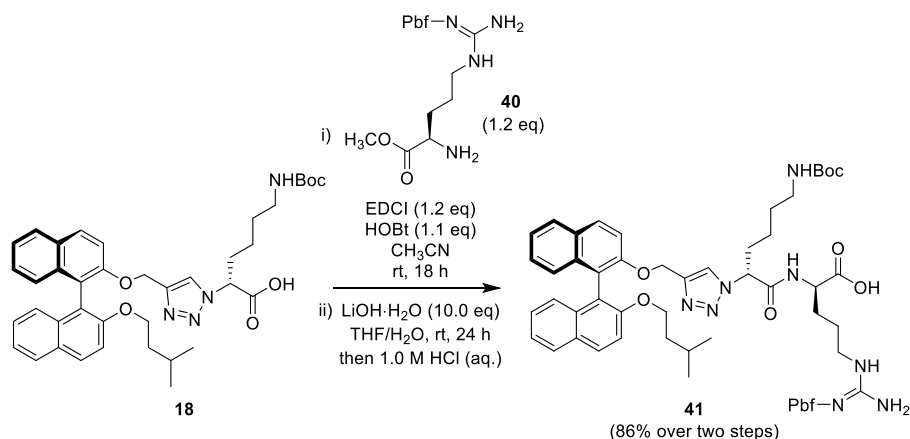
Entry	Compound	Aromatic Core	AA·HCl	R	Yield(%) <sup>a</sup>
1	<b>20</b>	Biphenyl	Lys		95
2	<b>21</b>	Biphenyl	Lys		94
3	<b>22</b>	Biphenyl	Lys		94

4	<b>23</b>	Biphenyl	Lys		92
5	<b>24</b>	Biphenyl	Lys		97
6	<b>25</b>	Biphenyl	Lys		93
7	<b>26</b>	Biphenyl	Arg		94
8	<b>27</b>	Biphenyl	Arg		87
9	<b>28</b>	Biphenyl	Arg		95
10	<b>29</b>	Biphenyl	Arg		60
11	<b>30</b>	Biphenyl	Arg		65
12	<b>31</b>	Biphenyl	Arg		84
13	<b>32</b>	Biphenyl	Arg		53
14	<b>33</b>	Biphenyl	Arg		79
15	<b>34</b>	Biphenyl	Arg		89
16	<b>35</b>	Biphenyl	Arg		81
17	<b>36</b>	Biphenyl	Arg		89
18	<b>37<sup>b</sup></b>	Biphenyl	Arg		86
19	<b>38</b>	( <i>S</i> )-Binaphthyl	Arg		87
20	<b>39</b>	( <i>S</i> )-Binaphthyl	Arg		49

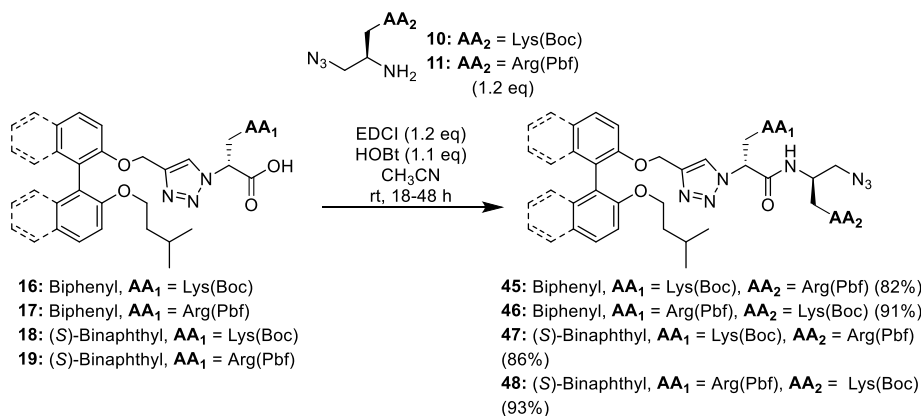
<sup>a</sup> Yields are reported over two steps.

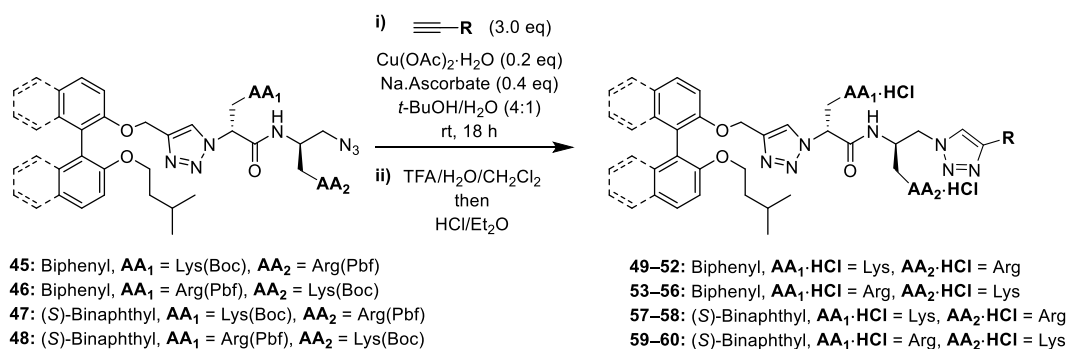
<sup>b</sup> *N,N*-disubstituted amide: two -**R** groups.

EDCI/HOBt peptide coupling of scaffold acid **18** with amino ester **40** [29] followed by base-promoted hydrolysis gave access to the Series **B** scaffold acid **41** (Scheme 4). The previously utilized two-step derivatization/side-chain deprotection sequence was then employed to achieve the Series **B** dicationic amphiphiles **42–44** (Scheme 5) as their di-hydrochloride salts.



The Series **C** scaffold azides **45–48** were assembled from scaffold acids **16–19** by EDCI/HOBT peptide coupling with the corresponding azido amine precursor (**10** or **11**) (Scheme 6). The resultant scaffold azides were then derivatized *via* CuAAC reaction and subjected to acidolytic side-chain *N*-deprotection to furnish the Series **C** dicationic amphiphiles **49–60** (Table 2) as their di-hydrochloride salts.

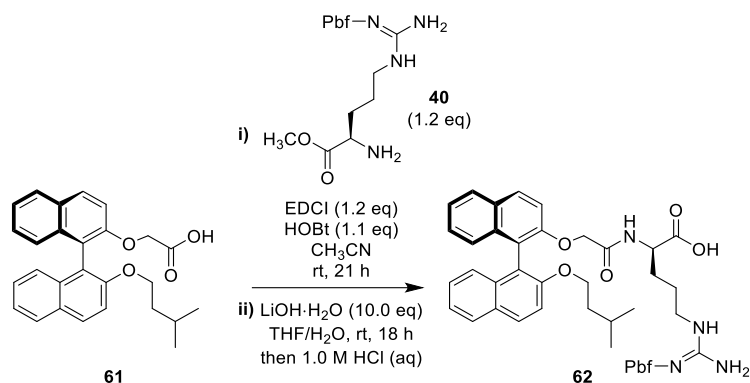


**Table 2.** Synthesis of the Series C dicationic amphiphiles.

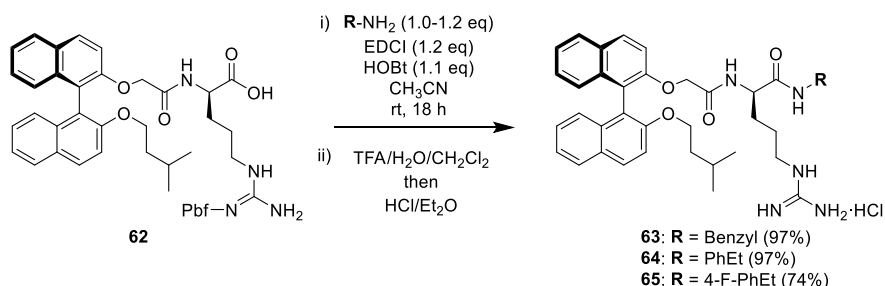
Entry	Compound	Aromatic Core	$\text{AA}_1 \cdot \text{HCl}$	$\text{AA}_2 \cdot \text{HCl}$	R	Yield(%) <sup>a</sup>
1	<b>49</b>	Biphenyl	Lys	Arg		95
2	<b>50</b>	Biphenyl	Lys	Arg		85
3	<b>51</b>	Biphenyl	Lys	Arg		94
4	<b>52</b>	Biphenyl	Lys	Arg		90
5	<b>53</b>	Biphenyl	Arg	Lys		84
6	<b>54</b>	Biphenyl	Arg	Lys		94
7	<b>55</b>	Biphenyl	Arg	Lys		97
8	<b>56</b>	Biphenyl	Arg	Lys		90
9	<b>57</b>	(S)-Binaphthyl	Lys	Arg		56
10	<b>58</b>	(S)-Binaphthyl	Lys	Arg		75
11	<b>59</b>	(S)-Binaphthyl	Arg	Lys		95
12	<b>60</b>	(S)-Binaphthyl	Arg	Lys		68

<sup>a</sup> Yields are reported over two steps.

In addition to the three main series of synthesized antibacterial biaryl 1,2,3-triazolyl peptidomimetics (i.e Series **A**, **B** and **C**), a small subset of non-triazole amphiphiles (Series **D**) was synthesized for comparison to the triazole-containing derivatives. The Series **D** scaffold acid **62** was obtained by EDCI/HOBt promoted peptide coupling reaction of acid **61** [34-35] with amino ester **40** [29] followed by ester hydrolysis with  $\text{LiOH} \cdot \text{H}_2\text{O}$  in  $\text{THF}/\text{H}_2\text{O}$  (Scheme 7). The scaffold acid **62** was then subjected to the same sequential, two-step derivatization procedure utilized for the Series **A** and **B** derivatives to achieve the Series **D** amphiphiles **63–65** as hydrochloride salts (Scheme 8).



**Scheme 7.** Synthesis of the Series **D** acid scaffold **62**.



**Scheme 8.** Synthesis of the Series **D** non-triazole derivatives **63–65**.

The  $^1\text{H}$  and  $^{13}\text{C}$  NMR spectra of specific amphiphilic derivatives (e.g. compound **23** – see Fig. S4 and S5) were found to exhibit rotameric resonance shouldering due to *syn*- and *anti*-amide and -carbamate rotamers (much akin to the previously synthesized cationic biaryl amphiphiles [28]). Evidence of rotameric entities amongst the biaryl peptidomimetics has previously been elucidated with variable temperature NMR experiments [28].

Compound **28** was produced in >1 gram quantities for use in an *in vivo* murine *C. difficile* model; the purity was confirmed to be >99% by reverse-phase analytical HPLC (Fig. S6).

## 2.2. Antibacterial activity evaluation

The synthesized peptidomimetic derivatives (Series **A**, **B**, **C** and **D**) were subjected to an antibacterial minimum inhibitory concentration (MIC) assay against a primary panel of Gram-positive pathogenic bacteria with vancomycin as a positive control; the MIC results are displayed in Tables 3–6. The compounds were then tested in an MIC assay against a secondary panel of Gram-negative pathogenic bacteria and MRSA at the Community for Open Antimicrobial Drug Discovery (CO-ADD) [44]. A cytotoxicity concentration ( $\text{CC}_{50}$ ) assay was also performed by CO-ADD; the synthesized compounds were tested at concentrations  $\leq 32$   $\mu\text{g/mL}$ . Vancomycin, colistin and tamoxifen were used as positive controls in the Gram-positive, Gram-negative and cytotoxicity assays, respectively. The CO-ADD antibacterial activities and  $\text{CC}_{50}$  values from Series **A**, **B**, **C** and **D** are displayed in Tables 7–10, respectively.

Initial MIC screening results indicated that reversal of the peptide backbone orientation to achieve a shorter synthetic pathway did not negatively impact the antibacterial efficacy of the amphiphilic molecules; both the monocationic (Series **A**) and dicationic (Series **B** and **C**) derivatives exhibited potent antibacterial activities against Gram-positive bacteria, with MIC values ranging from 2–16  $\mu\text{g/mL}$  against *S. aureus* (Tables 3, 4 and 5). Amongst the monocationic Series **A** compounds, the arginine derivatives (**26–39**) were consistently more active against Gram-positive pathogens than their lysine counterparts (**20–25**) (Table 3). The monocationic (*S*)-binaphthyl analogues **38** and **39** exhibited similar MIC values against the Gram-positive bacteria relative to their biphenyl counterparts **26** and **27** (i.e. within one MIC dilution). The arginine compound **28** was identified as the most potent monocationic derivative against *C. difficile* (MIC = 8  $\mu\text{g/mL}$ ) with strong activity against all other Gram-positive bacteria tested (MIC = 4  $\mu\text{g/mL}$ ) (Table 3). Most notably, *C. difficile* exhibited decreased

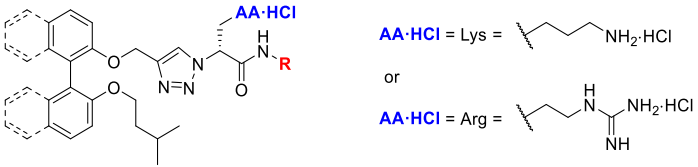
susceptibility to the monocationic compounds (**26–39**) relative to the other Gram-positive bacterial strains, displaying MIC values 2–8× fold less potent than the corresponding *S. aureus* MIC values (Table 3). Secondary MIC screening revealed that the monocationic derivatives lacked substantial activity against Gram-negative pathogens, with MIC values  $\geq 32$   $\mu\text{g/mL}$  for virtually all Series **A** compounds that were tested (Table 7); these results were found to be in agreement with previous studies [28].

The Series **B** dicationic amide analogues (**42–44**) displayed similar antibacterial efficacy against Gram-positive bacteria when compared to the monocationic Series **A** derivatives (Table 4). The presence of a second cationic residue endowed Gram-negative antibacterial efficacy to the cationic biaryl peptidomimetics, with MIC values of 8  $\mu\text{g/mL}$  against *A. baumannii* and 16  $\mu\text{g/mL}$  against *K. pneumoniae* and *P. aeruginosa* for the dicationic amide **44** (Table 8). As previously indicated [28], the addition of a second cationic moiety allows for increased electrostatic attraction to the anionic bacterial membrane and a more optimal amphiphilic structure, which likely explains the observed general increase in antibacterial efficacy.

Testing of the Series **C** dicationic bis-triazole derivatives (**49–60**) revealed potent antibacterial activity against both Gram-positive and Gram-negative bacterial pathogens (Tables 5 and 9, respectively). The Series **C** analogues displayed increased efficacy against *C. difficile* with MIC values of 8–16  $\mu\text{g/mL}$  exhibited by the majority of the compounds tested. The biphenyl Series **C** analogues (e.g. compounds **49–56**) displayed notably stronger antibacterial efficacy against Gram-negative bacteria than their (*S*)-binaphthyl counterparts (**57–60**) (Table 9); these results were in agreement with previous studies on related compounds [28]. The more soluble, less bulky biphenyl aromatic core may allow for easier penetration of the outer bacterial membrane to allow access to the cytoplasmic membrane, which could explain the increased efficacy observed against Gram-negative pathogens. Interestingly, the orientation of the two cationic residues was found to have little impact on antibacterial activity against Gram-positive pathogens (Table 5); however, the Lys-Arg orientation was markedly superior to the Arg-Lys orientation (i.e. 2–4× more potent) for the Gram-negative species *E. coli* and *A. baumannii* (Table 9).

Systematic variation on the hydrophobic termini was found to have a notable effect on the MIC values of the peptidomimetic amphiphiles; the least active Series **A** derivative was also the only monocationic *N,N*-disubstituted amide, indicating that too much steric bulk at the terminus resulted in a decrease in antibacterial activity. Furthermore, no one particular terminus was found to be superior, as the same terminus on different scaffolds gave widely different activities. For example, the monocationic lysine analogue **24** and arginine analogue **30** both contain a 4-CF<sub>3</sub>-benzyl amide terminus and therefore, the arginine analogue **30** was expected to exhibit stronger MIC values based upon previous findings; paradoxically, the lysine derivative **24** exhibited stronger MIC values (Table 3), indicating that the overall amphipathic conformation of the molecule was likely the dominant influencing factor, rather than the individual termini itself.

**Table 3.** Primary screening: antibacterial activities of Series **A** derivatives reported as MIC values ( $\mu\text{g/mL}$ ).



AA·HCl = Lys = CCCC(N)C(=O)N·HCl  
 or  
 AA·HCl = Arg = CCC(N)C(=O)N·HCl

Entry	Compound	Aromatic Core	AA	R	<i>S. aureus</i>		<i>E. faecalis</i>	<i>S. pneumoniae</i>	<i>C. difficile</i>	
					ATCC 29213	NCTC 10442 (MRSA)	ATCC 29212	ATCC 49619	ATCC 700057	132 (RT027)
1	<b>20</b>	Biphenyl	Lys	Bn	8	16	16	8	32	32
2	<b>21</b>	Biphenyl	Lys	PhEt	8	8	8	8	32	32
3	<b>22</b>	Biphenyl	Lys	Cy	8	16	16	8	16	32
4	<b>23</b>	Biphenyl	Lys	CH <sub>2</sub> Cy	8	8	8	8	16	32
5	<b>24</b>	Biphenyl	Lys	4-CF <sub>3</sub> -Bn	4	4	4	8	32	32
6	<b>25</b>	Biphenyl	Lys	4-F-PhEt	4	8	8	8	32	64
7	<b>26</b>	Biphenyl	Arg	Bn	4	8	8	4	32	64
8	<b>27</b>	Biphenyl	Arg	PhEt	2	2	4	4	8	32
9	<b>28</b>	Biphenyl	Arg	Cy	4	4	4	4	8	16
10	<b>29</b>	Biphenyl	Arg	CH <sub>2</sub> Cy	4	4	8	8	32	64
11	<b>30</b>	Biphenyl	Arg	4-CF <sub>3</sub> -Bn	16	16	16	32	128	128
12	<b>31</b>	Biphenyl	Arg	4-F-PhEt	4	4	4	4	64	64
13	<b>32</b>	Biphenyl	Arg	3,5-diF-Bn	8	8	8	16	32	32
14	<b>33</b>	Biphenyl	Arg	3-F-Phenyl	4	8	8	8	32	64
15	<b>34</b>	Biphenyl	Arg	3,5-diMeO-Phenyl	2	2	2	2	16	32
16	<b>35</b>	Biphenyl	Arg	Cyclopropyl	4	4	4	4	32	32
17	<b>36</b>	Biphenyl	Arg	Cyclopropylmethyl and Propyl <sup>a</sup>	16	32	32	8	64	128
18	<b>37</b>	Biphenyl	Arg	Cyclopentenyl	4	4	4	2	16	16
19	<b>38</b>	(S)-Binaphthyl	Arg	Bn	4	8	2	8	16	16
20	<b>39</b>	(S)-Binaphthyl	Arg	PhEt	8	8	4	16	16	64
21	Vancomycin	-	-	-	1	1	4	1	0.5	0.5

<sup>a</sup> *N,N*-disubstituted amide: two -R groups.

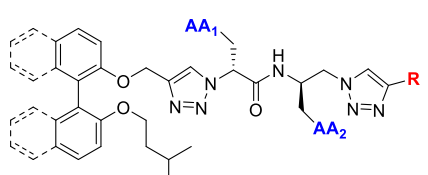
**Table 4.** Primary screening: antibacterial activities of Series **B** terminal amide derivatives reported as MIC values ( $\mu\text{g/mL}$ ).

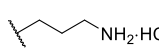
Entry	Compound	<b>R</b>	<i>S. aureus</i>		<i>E. faecalis</i>	<i>S. pneumoniae</i>	<i>C. difficile</i>	
			ATCC 29213	NCTC 10442 (MRSA)	ATCC 29212	ATCC 49619	ATCC 700057	132 (RT027)
1	<b>42</b>	Bn	8	8	8	8	16	16
2	<b>43</b>	PhEt	8	8	4	8	16	32
3	<b>44</b>	Piperidinyl <sup>a</sup>	8	8	8	8	16	32
4	Vancomycin	-	1	1	4	1	0.5	0.5

<sup>a</sup> *N,N*-disubstituted amide.

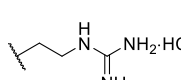


**Table 5.** Primary screening: antibacterial activities of Series C terminal triazole derivatives reported as MIC values ( $\mu\text{g/mL}$ ).

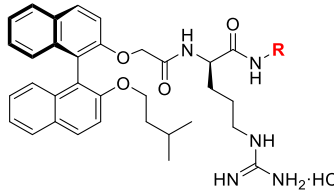


AA = Lys =   $\text{NH}_2 \cdot \text{HCl}$

or

AA = Arg =   $\text{NH}_2 \cdot \text{HCl}$

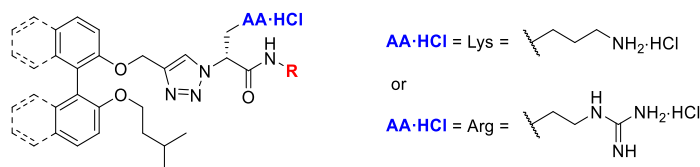
Entry	Compound	Aromatic Core	AA <sub>1</sub>	AA <sub>2</sub>	R	<i>S. aureus</i>		<i>E. faecalis</i>	<i>S. pneumoniae</i>	<i>C. difficile</i>	
						ATCC 29213	NCTC 10442 (MRSA)	ATCC 29212	ATCC 49619	ATCC 700057	132 (RT027)
1	<b>49</b>	Biphenyl	Lys	Arg	Bn	4	4	8	4	8	16
2	<b>50</b>	Biphenyl	Lys	Arg	PhEt	4	4	8	8	16	16
3	<b>51</b>	Biphenyl	Lys	Arg	Cy	16	16	16	32	64	128
4	<b>52</b>	Biphenyl	Lys	Arg	CH <sub>2</sub> Cy	4	4	4	8	16	16
5	<b>53</b>	Biphenyl	Arg	Lys	Bn	8	8	8	4	32	16
6	<b>54</b>	Biphenyl	Arg	Lys	PhEt	4	8	8	2	16	16
7	<b>55</b>	Biphenyl	Arg	Lys	Cy	8	8	8	2	8	16
8	<b>56</b>	Biphenyl	Arg	Lys	CH <sub>2</sub> Cy	4	4	4	2	8	16
9	<b>57</b>	( <i>S</i> )-Binaphthyl	Lys	Arg	PhEt	4	4	4	4	16	16
10	<b>58</b>	( <i>S</i> )-Binaphthyl	Lys	Arg	CH <sub>2</sub> Cy	4	4	4	4	16	16
11	<b>59</b>	( <i>S</i> )-Binaphthyl	Arg	Lys	PhEt	4	4	4	2	16	16
12	<b>60</b>	( <i>S</i> )-Binaphthyl	Arg	Lys	CH <sub>2</sub> Cy	4	4	4	2	8	8
13	Vancomycin	-	-	-	-	1	1	4	1	0.5	0.5

**Table 6.** Primary screening: antibacterial activities of Series **D** non-triazole derivatives reported as MIC values ( $\mu\text{g/mL}$ ).


The chemical structure shows a biphenyl core with two ether linkages. One ether is connected to a propyl chain, and the other is connected to a chain containing a secondary amide with an R group, and a primary amide with an NH<sub>2</sub> group. The primary amide is shown as a hydrochloride salt (NH<sub>2</sub>·HCl).

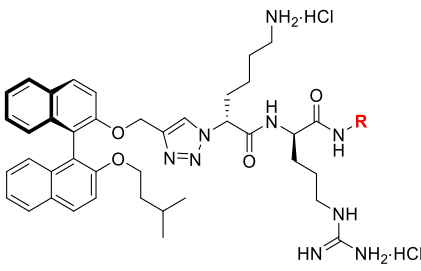
Entry	Compound	R	<i>S. aureus</i>		<i>E. faecalis</i>	<i>S. pneumoniae</i>	<i>C. difficile</i>	
			ATCC 29213	NCTC 10442 (MRSA)	ATCC 29212	ATCC 49619	ATCC 700057	132 (RT027)
1	<b>63</b>	Bn	2	2	2	2	8 <sup>a</sup>	8 <sup>a</sup>
2	<b>64</b>	PhEt	2	2	4	2	32	32
3	<b>65</b>	4-F-PhEt	>128	>128	>128	>128	>128	64
4	Vancomycin	-	1	1	4	1	0.5	0.5

<sup>a</sup> Compound **63** displayed an MIC value of 2  $\mu\text{g/mL}$  against *C. difficile* (M7404 – RT027) when tested at the Monash University laboratory.

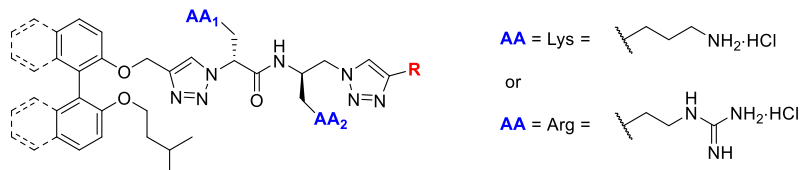
**Table 7.** Secondary screening: antibacterial activities of Series **A** derivatives reported as MIC values ( $\mu\text{g/mL}$ ).

Entry	Compound	Aromatic Core	AA	R	<i>S.</i>	<i>P.</i>	<i>K.</i>	<i>A.</i>	<i>E. coli</i>	Cytotoxicity
					<i>aureus</i> ATCC 43300 (MRSA)	<i>aeruginosa</i> ATCC 27853	<i>pneumoniae</i> ATCC 700603	<i>baumannii</i> ATCC 19606	ATCC 25922	(CC <sub>50</sub> ) (HEK-293) ATCC CRL-1573
1	<b>20</b>	Biphenyl	Lys	Bn	16	32	>32	32	>32	>32
2	<b>21</b>	Biphenyl	Lys	PhEt	8	>32	>32	32	>32	>32
3	<b>22</b>	Biphenyl	Lys	Cy	8	32	>32	32	>32	>32
4	<b>23</b>	Biphenyl	Lys	CH <sub>2</sub> Cy	8	>32	>32	32	>32	5.6
5	<b>24</b>	Biphenyl	Lys	4-F-PhEt	8	>32	>32	32	>32	>32
6	<b>25</b>	Biphenyl	Lys	4-CF <sub>3</sub> -Bn	8	>32	>32	16	>32	5.5
7	<b>26</b>	Biphenyl	Arg	Bn	8	>32	>32	32	>32	16.8
8	<b>27</b>	Biphenyl	Arg	PhEt	8	>32	>32	32	>32	17.9
9	<b>28</b>	Biphenyl	Arg	Cy	4	>32	>32	32	>32	19.7
10	<b>29</b>	Biphenyl	Arg	CH <sub>2</sub> Cy	4	>32	>32	>32	>32	16.9
11	<b>30</b>	Biphenyl	Arg	4-F-PhEt	16	>32	>32	>32	>32	>32
12	<b>31</b>	Biphenyl	Arg	4-CF <sub>3</sub> -Bn	16	>32	>32	>32	>32	19.1
13	<b>32</b>	Biphenyl	Arg	3,5-diF-Bn	16	>32	>32	>32	>32	22.9
14	<b>33</b>	Biphenyl	Arg	3-F-Phenyl	4	>32	>32	>32	>32	>32
15	<b>34</b>	Biphenyl	Arg	3,5-diMeO-Phenyl	8	>32	>32	>32	>32	21.6
16	<b>35</b>	Biphenyl	Arg	Cyclopropyl	8	>32	>32	>32	>32	12.2
17	<b>36</b>	Biphenyl	Arg	Cyclopropyl-methyl and Propyl <sup>a</sup>	32	>32	>32	>32	>32	20.0
18	<b>37<sup>b</sup></b>	Biphenyl	Arg	Cyclopentyl	8	>32	>32	>32	>32	19.7
19	<b>38</b>	( <i>S</i> )-Binaphthyl	Arg	Bn	8	>32	>32	>32	>32	16.5
20	<b>39</b>	( <i>S</i> )-Binaphthyl	Arg	PhEt	8	>32	>32	>32	>32	>32
21	Vancomycin	-	-	-	1	-	-	-	-	-
22	Colistin	-	-	-	-	0.25	0.25	0.25	0.125	-
23	Tamoxifen	-	-	-	-	-	-	-	-	13.1

<sup>a</sup> *N,N*-disubstituted amide: two -R groups.

**Table 8.** Secondary screening: antibacterial activities of Series **B** derivatives reported as MIC values ( $\mu\text{g/mL}$ ).


Entry	Compound	R	<i>S.</i>	<i>P.</i>	<i>K.</i>	<i>A.</i>	<i>E. coli</i>	Cytotoxicity
			<i>aureus</i>	<i>aeruginosa</i>	<i>pneumoniae</i>	<i>baumannii</i>	<i>E. coli</i>	(CC <sub>50</sub> )
			ATCC 43300 (MRSA)	ATCC 27853	ATCC 700603	ATCC 19606	ATCC 25922	(HEK-293) ATCC CRL-1573
1	<b>42</b>	Bn	4	32	32	32	>32	17.4
2	<b>43</b>	PhEt	2	32	16	8	>32	15.2
3	<b>44</b>	Piperidinyl <sup>a</sup>	2	16	16	8	32	16.8
4	Vancomycin	-	1	-	-	-	-	-
5	Colistin	-	-	0.25	0.25	0.25	0.125	-
6	Tamoxifen	-	-	-	-	-	-	13.1

<sup>a</sup> *N,N*-disubstituted amide.**Table 9.** Secondary screening: antibacterial activities of Series **C** derivatives, reported as MIC values ( $\mu\text{g/mL}$ ).


Entry	Compound	Aromatic Core	AA <sub>1</sub>	AA <sub>2</sub>	R	<i>S.</i>	<i>P.</i>	<i>K.</i>	<i>A.</i>	<i>E. coli</i>	Cytotoxicity
						ATCC 43300 (MRSA)	ATCC 27853	ATCC 700603	ATCC 19606	ATCC 25922	(HEK-293) ATCC CRL-1573
1	<b>49</b>	Biphenyl	Lys	Arg	Bn	4	16	32	16	8	17.1
2	<b>50</b>	Biphenyl	Lys	Arg	PhEt	2	8	16	8	8	16.4
3	<b>51</b>	Biphenyl	Lys	Arg	Cy	4	16	16	8	8	19.8
4	<b>52</b>	Biphenyl	Lys	Arg	CH <sub>2</sub> Cy	2	32	16	8	8	19.1
5	<b>53</b>	Biphenyl	Arg	Lys	Bn	8	16	32	32	>32	>32
6	<b>54</b>	Biphenyl	Arg	Lys	PhEt	4	16	16	32	16	>32
7	<b>55</b>	Biphenyl	Arg	Lys	Cy	4	8	16	16	16	>32
8	<b>56</b>	Biphenyl	Arg	Lys	CH <sub>2</sub> Cy	8	16	16	16	16	>32
9	<b>57</b>	( <i>S</i> )-Binaphthyl	Lys	Arg	PhEt	2	16	>32	8	>32	>32
10	<b>58</b>	( <i>S</i> )-Binaphthyl	Lys	Arg	CH <sub>2</sub> Cy	2	32	>32	8	>32	16.6
11	<b>59</b>	( <i>S</i> )-Binaphthyl	Arg	Lys	PhEt	4	32	>32	32	>32	>32
12	<b>60</b>	( <i>S</i> )-Binaphthyl	Arg	Lys	CH <sub>2</sub> Cy	32	32	>32	32	>32	>32
13	Vancomycin	-	-	-	-	1	-	-	-	-	-
14	Colistin	-	-	-	-	-	0.25	0.25	0.25	0.125	-
15	Tamoxifen	-	-	-	-	-	-	-	-	-	13.1

**Table 10.** Secondary screening: antibacterial activities of Series **D** non-triazole derivatives, reported as MIC values ( $\mu\text{g/mL}$ ).

Entry	Compound	<b>R</b>	<i>S.</i>	<i>P.</i>	<i>K.</i>	<i>A.</i>	<i>E. coli</i>	Cytotoxicity
			<i>aureus</i>	<i>aeruginosa</i>	<i>pneumoniae</i>	<i>baumannii</i>	<i>E. coli</i>	(CC <sub>50</sub> )
			ATCC 43300 (MRSA)	ATCC 27853	ATCC 700603	ATCC 19606	ATCC 25922	(HEK-293) ATCC CRL-1573
1	<b>63</b>	Bn	4	>32	>32	>32	>32	>32
2	<b>64</b>	PhEt	4	>32	>32	>32	>32	>32
3	<b>65</b>	4-F-PhEt	4	>32	>32	>32	>32	>32
4	Vancomycin	-	1	-	-	-	-	-
5	Colistin	-	-	0.25	0.25	0.25	0.125	-
6	Tamoxifen	-	-	-	-	-	-	13.1

### 2.3. Haemolysis Assay

Selected peptidomimetic derivatives were subjected to a haemolysis assay with sheep erythrocytes at concentrations of 5  $\mu\text{g/mL}$  and 50  $\mu\text{g/mL}$ ; UltraPure H<sub>2</sub>O was utilized as a positive control (i.e. set as 100% haemolysis) and the results are displayed in Table 11.

**Table 11.** Percent haemolysis assay for selected derivatives from Series **A–D**.

Haemolysis Assay		
Compound	Testing Concentration	
	5 $\mu\text{g/mL}$	50 $\mu\text{g/mL}$
<b>23</b>	0.0%	98.0%
<b>28</b>	1.4%	81.8%
<b>39</b>	0.1%	55.2%
<b>50</b>	1.4%	12.6%
<b>56</b>	1.6%	33.7%
<b>57</b>	1.5%	75.2%
<b>60</b>	1.8%	71.5%
<b>63</b>	0.3%	100.5%

When tested at the lower testing concentration of 5  $\mu\text{g/mL}$ , the peptidomimetic compounds exhibited minimal haemolysis (i.e. <2%). The tested monocationic compounds **23**, **28**, **39**, and **63** displayed strong haemolytic activity (>50%) at the higher testing concentration, as expected due to their unoptimized cationic/hydrophobic ratio [28]. Gratifyingly, the biphenyl bis-triazole derivatives **50** and **56** exhibited substantially reduced haemolysis, with compound **50** displaying <13% haemolysis at the higher testing concentration. The corresponding (*S*)-binaphthyl analogues **57** and **60** exhibited higher levels of haemolysis relative to their biphenyl counterparts **50** and **56**, respectively. These findings were expected, as it has previously been shown that an increase in the ratio of cationic-to-hydrophobic substituents results in an increase in selectivity for the anionic bacterial membrane over the zwitterionic mammalian membrane [28]. Interestingly, the obtained cytotoxicity (CC<sub>50</sub>) values (Tables 7–10) did not always correlate with the haemolysis data; compound **56** was not cytotoxic at  $\leq 32$   $\mu\text{g/mL}$ , whereas

compound **50** exhibited a  $CC_{50}$  of 16.4  $\mu\text{g/mL}$ . The opposite pattern was observed amongst the haemolysis data, wherein compound **56** was found to be approximately 2 $\times$  more haemolytic than compound **50**.

#### 2.4. Comparative solubility assay

Initial *in vivo* murine studies revealed poor solubility in 10% DMSO/H<sub>2</sub>O for some of the (*S*)-binaphthyl analogues, so a comparative solubility assay was developed to ascertain the relative solubilities of the synthesized peptidomimetic compounds.

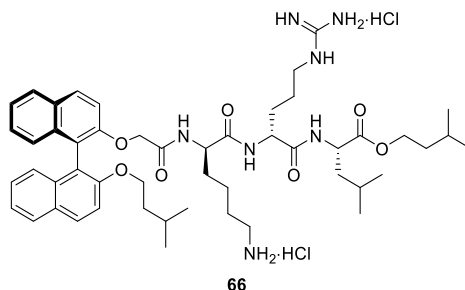


**Fig. 5.** Prototypical biarylpeptidomimetic compound **66**.

The prototypical biarylpeptidomimetic **66** [33] (Fig. 5) was used as the standard for solubility comparison and all other compounds were compared to this compound. The compound of interest (5.0 mg) was fully dissolved in DMSO (50  $\mu\text{L}$ ) and then H<sub>2</sub>O aliquots (5  $\mu\text{L}$ ) were added with adequate manual agitation in between additions. Addition of H<sub>2</sub>O was continued until a persistent turbidity and cloudiness was apparent that did not fade after agitation. Compound **66** precipitated after the addition of 15  $\mu\text{L}$  H<sub>2</sub>O; compounds that required twice as much water were effectively two times more soluble than compound **66** (i.e. solubility ratio = 2). The solubility assay was performed on a varied sample of the synthesized compounds to ascertain which structural elements were beneficial for solubility (Table 12).

**Table 12.** Comparative solubility assay data and CLogP values for selected compounds.

Solubility Assay Data			
Compound	H <sub>2</sub> O ppt. vol ( $\mu\text{L}$ )	Solubility Ratio (Compound : compound <b>66</b> )	CLogP
<b>66</b>	15	1	7.47
<b>1</b>	45	3	4.6
<b>23</b>	>200 <sup>NP</sup>	>13.3 <sup>NP</sup>	5.81
<b>28</b>	30	2	3.77
<b>51</b>	30	2	4.07
<b>56</b>	55	3.67	4.60
<b>60</b>	15	1	6.94
<b>63</b>	15	1	5.82
<b>67</b>	45	3	5.76
<b>68</b>	15	1	6.50
<b>69</b>	60	4	4.07

<sup>NP</sup> = No precipitation observed.

Comparison of the CLogP value and a compound's measured solubility revealed no definitive correlation between the two factors. As expected, the biphenyl derivatives were much more soluble than their corresponding (*S*)-binaphthyl analogues – for example, the biphenyl analogue **56** was almost four times more soluble than its (*S*)-binaphthyl counterpart **60** (Table 12). Compounds that contained a single lysine amino acid side-chain (e.g. compound **23**) were found to be substantially more soluble than the corresponding arginine containing analogues

(e.g. compound **28**); an alternative precipitation procedure (General Procedure D) was required for synthesis of the mono-lysine derivatives due to their increased solubility in Et<sub>2</sub>O.

Notably, no one particular orientation of amino acid residues amongst the dicationic derivatives was found to give rise to increased solubility, as the solubility was likely reliant on multiple complex factors (e.g. scaffold shape, hydrogen bonding, solvent effects and overall conformation).

The solubility ratio data allowed for the selection of compounds for the *in vivo* mouse model of CDI with varying solubilities so that the effect of solubility on the drug's administration, efficacy and pharmacokinetic parameters could be observed. Compounds required a solubility ratio of three or greater to prevent immediate precipitation and flocculation of the compound after dilution of the DMSO stock solution with H<sub>2</sub>O.

### 2.5. *In vivo* murine model for treatment of CDI

Compounds from this study and previous studies [28-29] were selected for use in a murine *in vivo* *C. difficile* infection treatment model [45] based upon their MIC values against *C. difficile* and varying solubility parameters. An initial study with two compounds (Fig. 6) was performed followed by a second study with four compounds (Fig. 7).

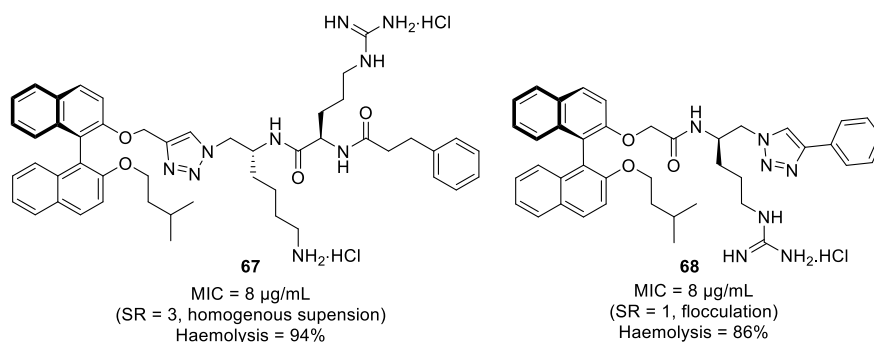


**Fig. 6.** Compounds **67** [28] and **68** [29] utilized in the initial *in vivo* CDI model; MIC values against *C. difficile* are displayed in µg/mL. The solubility ratio (SR) of each compound relative to compound **66** is displayed with a qualitative observation of the solubilisation in 10% DMSO. Haemolysis = Percent (%) haemolysis at 50 µg/mL.

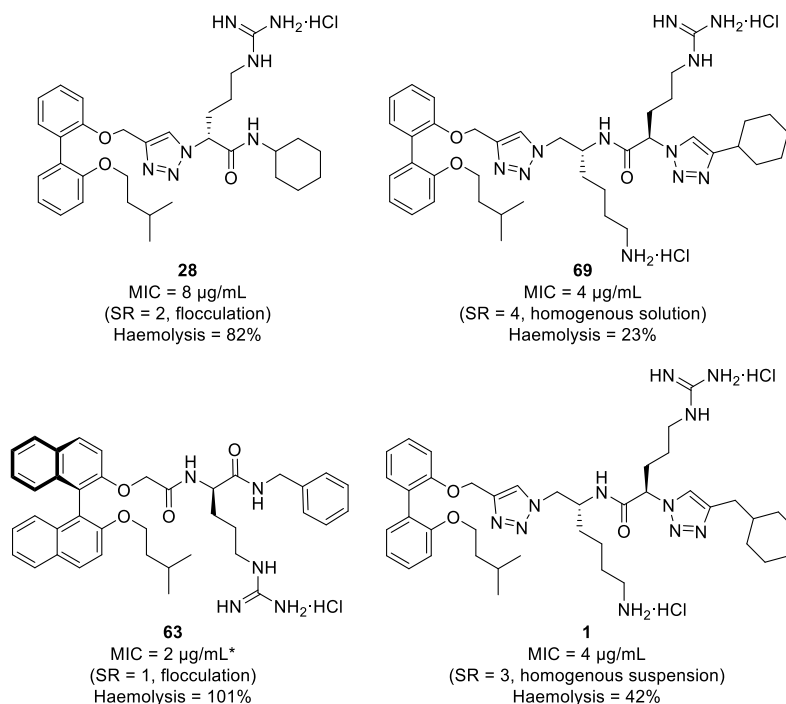


**Fig. 7.** Selected compounds **28**, **63**, **69** [28] and **1** [28] utilized in the secondary *in vivo* CDI model; MIC values against *C. difficile* are displayed in µg/mL. The solubility ratio (SR) of each compound relative to compound **66** is displayed with a

qualitative observation of the solubilisation in 10% DMSO. Haemolysis = Percent (%) haemolysis at 50 µg/mL. \*Compound **63** displayed an MIC value of 2 µg/mL against *C. difficile* M7404 at the Monash University laboratory.

Cohorts of mice (n = 4–5) were pre-treated with an antibiotic cocktail to induce susceptibility to bacterial infection followed by infection with *C. difficile* (ribotype 027 – strain M7404 [46]) spores *via* oral gavage. Each cohort was then administered either a test compound, vancomycin or a 10% DMSO control by oral gavage every 12 h starting from six hours after the initial infection. The mice were then monitored for weight loss, survival and physiological parameters for up to four days. Tables defining the physiological parameter scoring rubrics can be found in the supplementary information (Tables S1–S3).

The initial *in vivo* murine CDI model was performed on compounds **67** and **68** with vancomycin and 10% DMSO as positive and negative controls, respectively (Fig. 8). At twenty-four hours post-infection, compound **67** appeared to be protecting the mice from disease; these mice had the least diarrhoea (as shown by the fecal consistency score and cage appearance score) and their appearance was significantly better than the 10% DMSO control mice (Fig. 8). Furthermore, these mice showed a 50% survival rate (2/4 mice) compared to 0% survival in the 10% DMSO group, although this was not statistically significant due to the small sample size (Fig. 8a). These results clearly show that compound **67** exhibited a notable positive effect in the treatment of CDI. Compound **68** exhibited poor solubility during the *in vivo* trial, as the compound was found to precipitate during preparation in a 10% DMSO solution; these results prompted a review of the solubility parameters before further *in vivo* studies were conducted.

A secondary *in vivo* murine CDI model was performed with compounds **28**, **63**, **69** and **1**; these four compounds were selected due their potent *in vitro* activity against *C. difficile* in conjunction with their varying solubility profiles and structural motifs. At twenty-four hours post-infection, compound **28** appeared to be protecting the mice from disease; these mice had the least amount of weight loss at day 1 (not statistically significant) and they had the least amount of diarrhoea, as shown by the fecal consistency score and cage appearance score (Fig. 9). Furthermore, these mice physically looked the healthiest with 4/5 mice surviving until day 2, compared with only 2/5 mice from the 10% DMSO control cage surviving until day 2. Notably, compound **63** seemed to make the disease worse, as all 5 mice in this cohort were euthanized at 1 day post-infection and were worse than the 10% DMSO control mice in appearance (statistically significant), diarrhoea and weight loss (Fig. 9). Unfortunately, none of the compounds were able to fully protect the mice and all mice succumbed to infection by day 2 post-infection. Compound **28** performed significantly better than the DMSO control, providing some evidence of *in vivo* efficacy.

While the results from the *in vivo* murine CDI models were promising, the observed efficacy did not correlate with the *in vitro* MIC activities. For example, compound **28** exhibited the weakest MIC activity against *C. difficile* amongst the secondary *in vivo* trial derivatives; yet this compound performed better than the more potent analogues **63**, **69** and **1**. The non-triazole compound **63** exhibited the strongest *in vitro* MIC activity against *C. difficile*, yet it performed the worst out of the tested compounds. Unexpectedly, the more potent, more soluble and less haemolytic dicationic compounds **1** and **69** failed to perform as well as compound **28** (Fig. 9); there were no apparent correlations between a compound's MIC value, solubility, haemolysis and *in vivo* efficacy against CDI.

Overall, both compounds **67** and **28** displayed significant evidence of *in vivo* efficacy in the treatment of CDI, although further work and experiments are required to optimize the *in vivo* efficacy to a more reliable level.

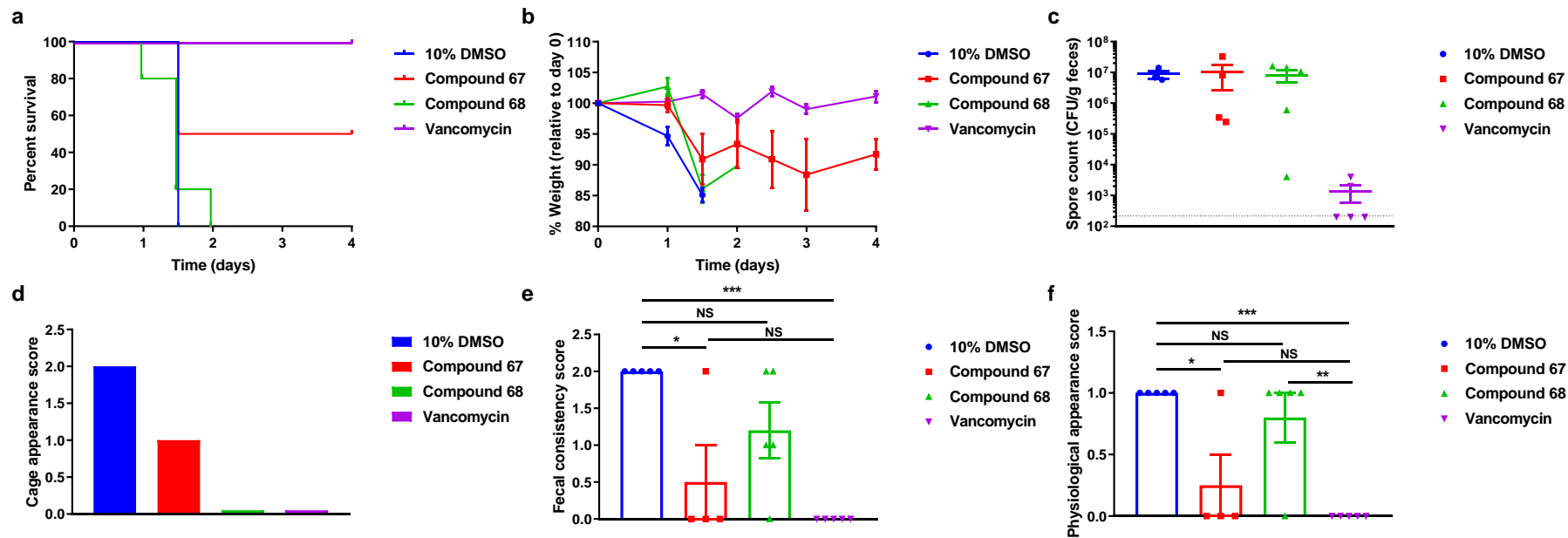


**Fig. 8. Initial *in vivo* murine CDI model.** C57BL/6J mice (n = 4–5 per group) were infected with 10<sup>5</sup> spores of *C. difficile* strain M7404 prior to treatment with DMSO, compound **67**, compound **68** or vancomycin and monitored daily for survival (**a**) and weight loss (**b**). Fecal spore load at 1 day post-infection was determined by plating (**c**). Data are presented as CFU/gram feces, with each point representing a single mouse. The dotted line represents the limit of detection of the assay. Mouse cages were scored on day 1 post-infection for appearance (**d**) and mice were individually assessed for fecal consistency (**e**) and physiological appearance (**f**). Data represent the mean ±S.E.M. and statistical significance was assessed using a log-rank (Mantel-Cox) test or one-way ANOVA with a post-hoc Tukey’s multiple comparison test. \* indicates *P* < .05; \*\* indicates *P* < .01; \*\*\* indicates *P* < .001; NS = not significant.



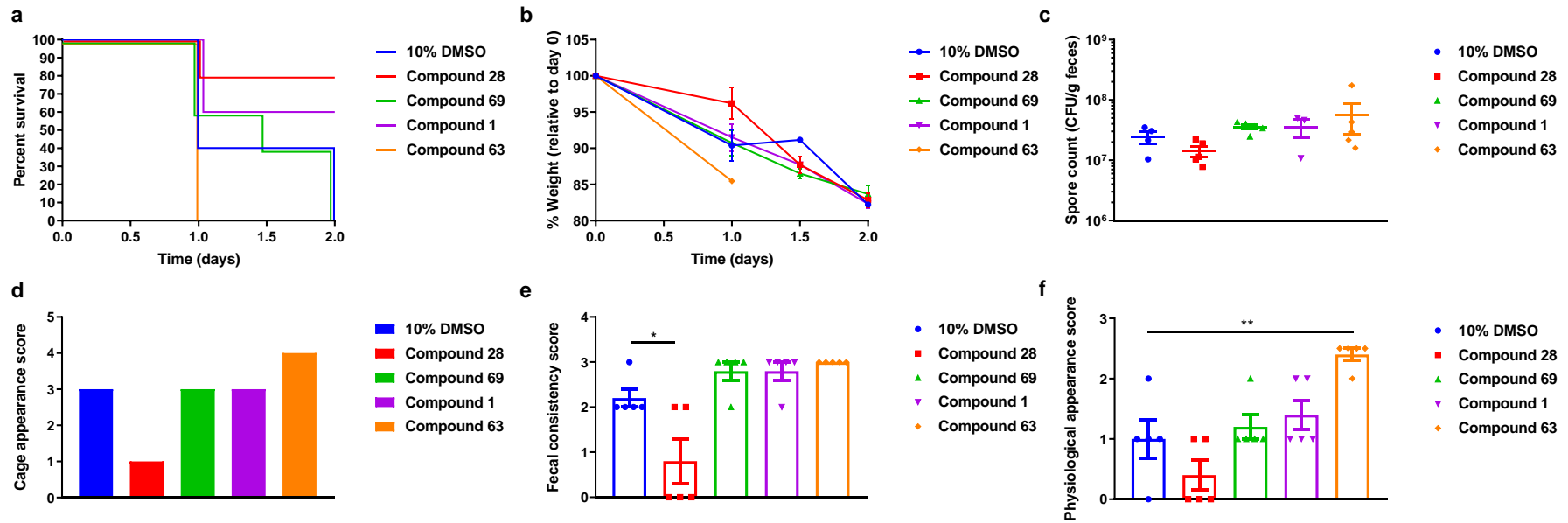


**Fig. 9. Secondary *in vivo* murine model of CDI.** C57BL/6J mice ( $n = 5$  per group) were infected with  $10^5$  spores of *C. difficile* strain M7404 prior to treatment with DMSO, compound 28, compound 69, compound 1 or compound 63 and monitored daily for survival (a) and weight loss (b). Fecal spore load at 1 day post-infection was determined by plating (c). Data are presented as CFU/gram feces, with each point representing a single mouse. Mouse cages were scored on day 1 post-infection for appearance (d) and mice were individually assessed for fecal consistency (e) and physiological appearance (f). Data represent the mean  $\pm$ S.E.M. and statistical significance was assessed using a log-rank (Mantel-Cox) test or one-way ANOVA with a post-hoc Tukey's multiple comparison test. \* indicates  $P < .05$ ; \*\* indicates  $P < .01$ .

## 2.6. Pharmacokinetics assay

Since CDI chemotherapeutics are required to stay in the GI tract to treat the infection, systemic absorption of the target antibiotic drug is not desirable. Therefore, pharmacokinetic analysis was performed on the blood and feces of mice that were infected with *C. difficile* and treated with lead compound **67** in the initial murine model of CDI (Section 2.5).

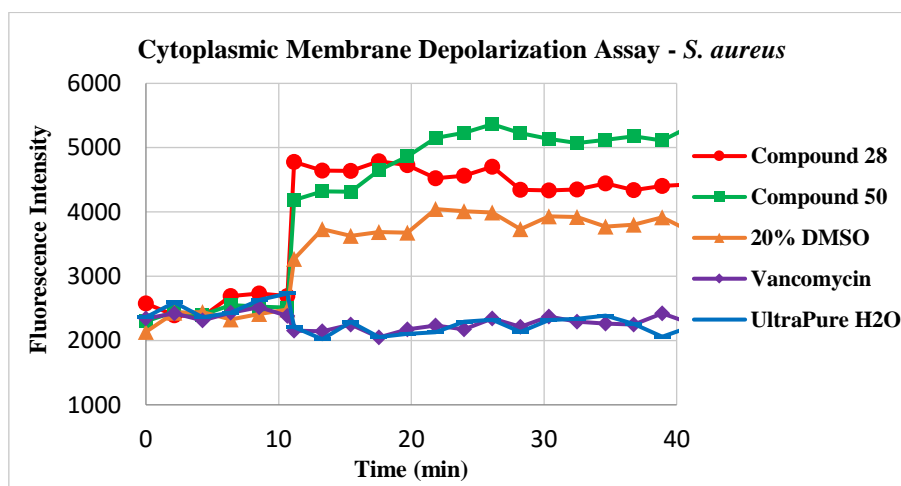
To ascertain the presence of compound **67** in the blood and feces, an extraction/analysis procedure employing low-resolution mass spectrometry (LRMS) was developed and utilized (Section 4.6). The mouse blood was diluted with PBS and then extracted with CH<sub>2</sub>Cl<sub>2</sub> (× 2); the feces was extracted with CH<sub>2</sub>Cl<sub>2</sub> (× 1). Concentration of the extracts and LRMS analysis of the residues revealed the presence of the drug (i.e. the doubly-protonated molecular ion,  $m/2 = 421 = [M + 2H]^{2+}$ ) in the feces; whereas no drug could be found in the blood. To ensure the procedure was viable, mouse blood from an untreated cohort was doped to achieve a final concentration of compound **67** equivalent to an average 25 g mouse absorbing 1% of the total dose into its bloodstream – the drug was readily detected in the doped mouse blood, verifying the validity of the extraction protocol.

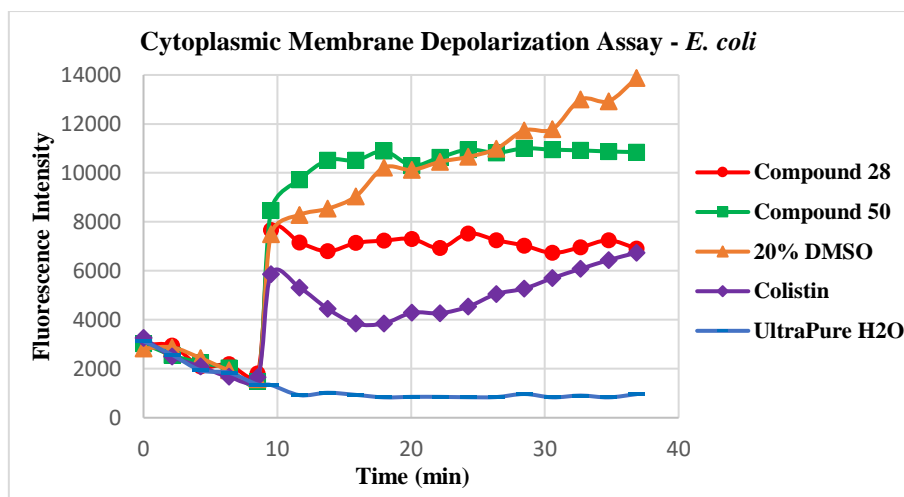
These findings confirm that compound **67** was not absorbed systemically into the bloodstream by the mice; following oral administration, the drug clearly stayed in the GI tract (i.e. feces).

## 2.7. Cytoplasmic membrane depolarization assay

A cytoplasmic membrane depolarization assay with 3,3'-dipropylthiadicarbocyanine (diSC<sub>3</sub>(5)) fluorescent dye [37, 47] was performed on compounds **28** and **50** against *S. aureus* (ATCC 29213) and *E. coli* (NCTC 10418) as described previously [28] to investigate the molecular mode of action. Compounds **28** and **50** were observed to strongly disrupt the electrochemical gradient of *S. aureus* at a testing concentration of 32 µg/mL (i.e. 8 × MIC) (Fig. 10, top). DMSO (20% aq.) was utilized as a positive control, resulting in a significant increase in observed fluorescence for both *S. aureus* and *E. coli* (Fig. 10). UltraPure H<sub>2</sub>O and vancomycin (for *S. aureus* only) were employed as negative controls and they failed to generate any increase in fluorescence. Furthermore, both compounds **28** and **50** were shown to depolarize the cytoplasmic membrane of *E. coli* when tested at 64 µg/mL (i.e. ≤8 × MIC), as shown by a large increase in the observed fluorescence (Fig. 10, bottom); the compounds elicited substantially stronger fluorescence than the positive control, colistin.

These results further confirm the previously elucidated membrane disruption mechanism inherent to these amphiphilic peptidomimetics [28].

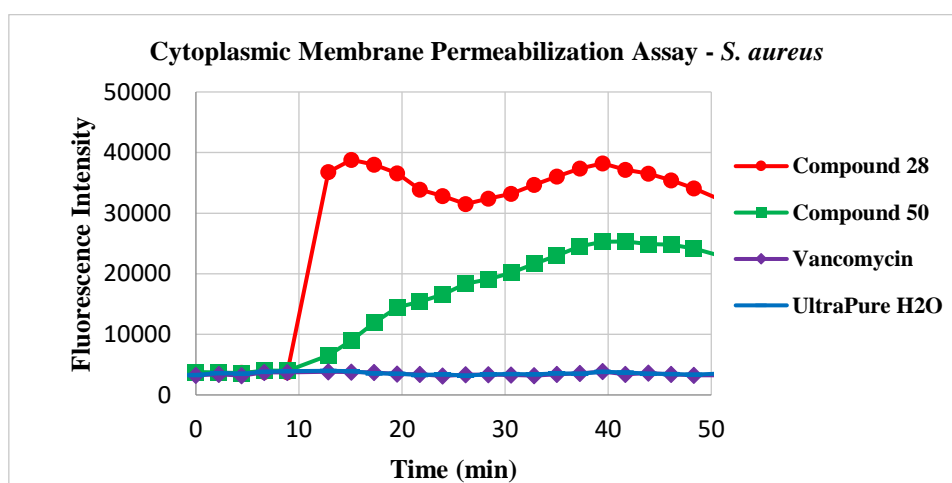




**Fig. 10** – Cytoplasmic membrane depolarization assays for compounds **28** and **50** tested at 32  $\mu\text{g}/\text{mL}$  against *S. aureus* (top) and 64  $\mu\text{g}/\text{mL}$  against *E. coli* (bottom). Vancomycin tested at 8  $\mu\text{g}/\text{mL}$  ( $8 \times \text{MIC}$ ) and colistin tested at 4  $\mu\text{g}/\text{mL}$  ( $32 \times \text{MIC}$ ).

### 2.8. Cytoplasmic membrane permeabilization assay

A cytoplasmic membrane permeabilization assay with propidium iodide [47-48] was conducted with compounds **28** and **50** against *S. aureus* and *E. coli* as previously described [28]. Compounds **28** and **50** exhibited a strong increase in fluorescence ( $>500\%$ ) in the assay against *S. aureus*, indicating permeabilization of the cellular membrane (Fig. 11, top). The negative controls vancomycin and UltraPure H<sub>2</sub>O failed to give an increase in fluorescence, as expected. As observed previously [28], the monocationic derivative **28** displayed a faster and stronger increase in fluorescence compared to the dicationic compound **50**; the monocationic analogue **28** took approximately 10 min to reach maximal fluorescence while the dicationic derivative **50** took approximately 40 min (Fig. 11, top). These results further confirm that the smaller, monocationic peptidomimetics likely permeabilize the cytoplasmic membrane of *S. aureus* more rapidly and effectively than the larger, dicationic derivatives. Permeabilization of the cytoplasmic membrane of *E. coli* by the peptidomimetics **28** and **50** was comparable to the permeabilization seen with the positive control, colistin (as indicated by the observed fluorescence) – yet this increase in fluorescence was notably reduced and slower (Fig. 11, bottom) relative to the fluorescence increase seen with *S. aureus*. This reduction in membrane permeabilization efficacy against *E. coli* is likely a result of the resilient outer membrane that is inherent to Gram-negative bacteria.



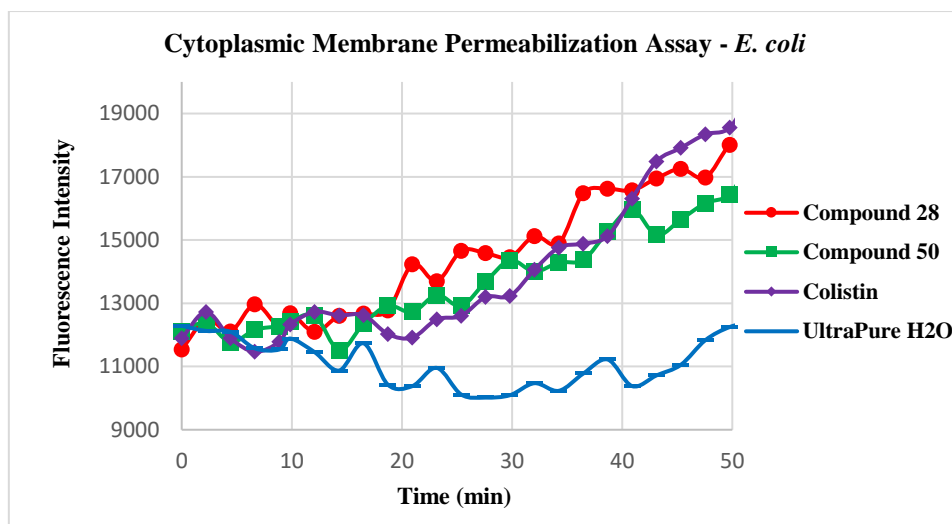


**Fig. 11** – Cytoplasmic membrane permeabilization assays for compounds **28** and **50** tested at 32  $\mu\text{g}/\text{mL}$  against *S. aureus* (top) and *E. coli* (bottom). Vancomycin was tested at 8  $\mu\text{g}/\text{mL}$  ( $8 \times \text{MIC}$ ) and colistin was tested at 4  $\mu\text{g}/\text{mL}$  ( $32 \times \text{MIC}$ ).

### 3. Conclusion

A simplified, modular synthetic pathway was employed to furnish thirty-eight novel cationic biaryl 1,2,3-triazolyl amphiphilic peptidomimetics. Nine variable scaffolds were developed and subsequently derivatized into twenty monocationic amide analogues (**A**), three dicationic amide analogues (**B**), twelve dicationic bis-triazole analogues (**C**) and three non-triazole analogues (**D**). The late-stage divergent methodology utilized the robust CuAAC and peptide coupling reactions to give facile synthetic access to the small library of antibacterial derivatives. Furthermore, the optimized synthetic pathway allowed access to the antibacterial scaffolds with substantially reduced synthetic labour. The synthesized compounds were found to exhibit potent antibacterial efficacy *in vitro* against a broad range of pathogenic Gram-positive and Gram-negative bacteria.

Compounds **28** and **67** exhibited significant evidence of *in vivo* efficacy in the murine CDI treatment models; further investigation into the structural and biological parameters affecting the *in vivo* efficacy of these antibacterial peptidomimetics is warranted, as the observed *in vitro* efficacy does not translate directly into *in vivo* efficacy. Preliminary pharmacokinetics assay results indicate that compound **67** is not absorbed systemically and that the compound remains in the GI tract following oral administration. Haemolytic testing revealed a correlation between an increased hydrophobic/cationic ratio and increased haemolytic activity; notably, compound **50** was found to exhibit substantially reduced haemolysis (<13%) relative to the majority of the tested analogues. Membrane disruption assay results strongly suggest a membrane-active mode of action for the amphiphilic peptidomimetics. A comparative solubility assay was developed that allowed for the identification of structural moieties that influenced the aqueous solubility of the synthesized peptidomimetics.

Identification of the parameters influencing the *in vivo* efficacy (e.g. solubility and membrane selectivity/haemolytic activity) against *C. difficile* will allow for the rational design and development of future antibacterial peptidomimetics with promising potential for use as chemotherapeutics in the treatment of CDI.

## 4. Experimental section

### 4.1. General information

#### Synthesis

Unless stated otherwise, all solvents and chemicals were laboratory or reagent grade and were purchased from commercial sources. All chemicals were used as received. Water was purified *via* Millipore filtration prior to use. HOBt and propargyl bromide were purchased with added stabilizers (10% w/w H<sub>2</sub>O and 20% w/w toluene, respectively); therefore, the quantities required for reactions were adjusted accordingly and are reflected in the reagent masses reported in the experimental (whereas the reported mmol quantities reflect the true quantity of chemical). All reactions were conducted under normal atmosphere and cold reaction temperatures were obtained by an ice bath (0 °C) or ice/salt bath (-10 °C). Heating of reactions was performed with a paraffin oil bath. Small quantities of liquid reagents were measured and added to reactions *via* syringe or autopipette. Unless otherwise noted, all filtrations were conducted as vacuum filtration through a sintered glass funnel (medium porosity). Vacuum filtration was achieved with the aid of a water aspirator. Solvent removal *via* concentration was performed on a rotary evaporator under reduced pressure. All solvent mixtures are expressed in terms of volume ratio (i.e. v/v). Thin layer chromatography (TLC) was performed on aluminium-backed SiO<sub>2</sub> gel plates (F<sub>254</sub> grade - 0.20 mm thickness). Visualization was achieved with UV light, ninhydrin stain or cerium ammonium molybdate stain. Flash chromatography was performed on SiO<sub>2</sub> gel 60 with positive air pressure. All synthesized compounds were dried under high vacuum (< 1 mbar) before determination of chemical yields and spectroscopic characterization.

#### Characterization and analysis

<sup>1</sup>H NMR spectra were recorded on a Bruker Avance 400 (400 MHz), a Varian VNMRs PS54 500 (500 MHz), a Varian Inova 500 (500 MHz) or a Varian Mercury 300 (300 MHz) NMR spectrometer. Chemical shifts are reported in ppm and were measured relative to the internal standard. Samples were dissolved in CDCl<sub>3</sub> (with TMS as the internal standard - 0.00 ppm), CD<sub>3</sub>OD (solvent resonance as internal standard - 3.31 ppm) or DMSO-*d*<sub>6</sub> (solvent resonance as internal standard - 2.50 ppm). The <sup>1</sup>H NMR data is reported as follows: chemical shift, multiplicity (s = singlet, d = doublet, t = triplet, q = quartet, dt = doublet of triplets, m = multiplet, br = broad), coupling constants (Hz) and integration. <sup>13</sup>C NMR spectra were recorded on a Bruker Avance 400 (101 MHz), a Varian VNMRs PS54 500 (126 MHz), a Varian Inova 500 (126 MHz) or a Varian Mercury 300 (75 MHz) NMR spectrometer with complete <sup>1</sup>H decoupling. Chemical shifts are reported in ppm and were measured relative to the internal standard. Samples were dissolved in CDCl<sub>3</sub> (solvent resonance as the internal standard - 77.16 ppm), CD<sub>3</sub>OD (solvent resonance as the internal standard - 49.20 ppm) or DMSO-*d*<sub>6</sub> (solvent resonance as internal standard - 39.50 ppm). <sup>1</sup>H and <sup>13</sup>C NMR assignments were confirmed by analysis of NMR APT, gCOSY, gHSQC, gHMBC and/or zTOCSY experiments. Ambiguous degenerate carbon resonances are marked with a single asterisk \* (representing two carbons) or a double asterisk \*\* (representing three or more carbons) for clarity. Carbon resonances that required 2-D NMR analysis for assignment (i.e. not observed *via* 1-D <sup>13</sup>C NMR analysis) are marked with the label “*observed by gHMBC*” or “*observed by gHSQC*”. NMR spectra were processed, analysed and prepared with MestReNova (version 6.0) NMR software. Low-resolution mass spectra (LRMS) were obtained *via* electrospray ionization (ESI) on a Shimadzu LC-2010 mass spectrometer. LRMS data was recorded as the ion mass/charge ratio (*m/z*) with the corresponding relative abundance as a percentage. High-resolution mass spectrometry (HRMS) was performed on a Waters Quadrupole-Time of Flight (QTOF) Xevo spectrometer *via* ESI and with Leucine-Enkephalin as an internal standard. All mass spectrometry samples were dissolved in high-performance liquid chromatography (HPLC) grade MeOH (containing <1% formic acid for ionization). Optical rotations were measured on a Jasco P-2000 polarimeter with a 10 cm path length; rotation values ( $\alpha$ ) are expressed in units of “deg cm<sup>3</sup> g<sup>-1</sup> dm<sup>-1</sup>” with concentration (*c*) expressed in units of “g/100 mL”. Solid-state infrared spectroscopy was performed on a Shimadzu IRAffinity-1 FTIR spectrometer in combination with a MIRacle 10 Single Reflection Attenuated Total Reflectance accessory outfitted with a 1.5 mm round diamond crystal. IR peaks are reported as the wavenumber ( $\nu_{\max}$  in cm<sup>-1</sup>) of the maximum absorption. Analytical HPLC was performed on a Phenomenex Synergi 4u Fusion-Reverse Phase 80Å column ( $\phi$  = 4.6 × 150 mm) with detection at  $\lambda$  = 215 nm and H<sub>2</sub>O/CH<sub>3</sub>CN (both containing 0.1% TFA) as the mobile phase.

### **Notes and other considerations**

Known reagents that were not available commercially were prepared according to the literature procedures cited within the supplementary information. The experimental section contains a representative synthesis of final compound **28** utilizing the general synthetic procedures outlined in Section 4.2; the synthetic and characterization data for all other compounds can be found within the supplementary information. Synthesized compounds that contain the (*S*)-isopentyloxybinaphthalene fragment and some chiral compounds that contain the isopentyloxybiphenyl fragment exhibited a pair of diastereotopic methyl (-CH<sub>3</sub>) groups on the terminus of the isopentyl substituent; these carbons are consistently referred to as C4'' and C5''. Importantly, these two carbons (and associated protons) would sometimes exhibit distinct NMR chemical shifts due to the chiral environment imposed by the amino acid residue(s) (for all derivatives) and/or the adjacent (*S*)-binaphthyl moiety (for (*S*)-binaphthyl derivatives only).

#### **4.2. General synthetic procedures**

##### **General Procedure A: Copper catalyzed azide-alkyne cycloaddition**

To a reaction vessel charged with the azide (1.0 eq), alkyne (2.0 – 3.0 eq), Cu(OAc)<sub>2</sub>·H<sub>2</sub>O (0.2 eq), and sodium ascorbate (0.4 eq) was added *t*-BuOH (20 mL/mmol azide) and H<sub>2</sub>O (5 mL/mmol azide). The mixture was initially sonicated for < 1 min followed by vigorous stirring at rt (unless noted otherwise) for the specified time. The reaction mixture was diluted with EtOAc (20 mL for reactions that contained ≤ 1.0 mmol azide or 20 mL/mmol azide for larger scale reactions) and washed with an equivalent volume of saturated aqueous NH<sub>4</sub>Cl solution (e.g. 20 mL). The organic phase was dried (MgSO<sub>4</sub>), filtered, concentrated and the residue was subjected to flash chromatography over SiO<sub>2</sub> gel to afford the desired 1,4-disubstituted-1,2,3-triazole product.

##### **General Procedure B: Amide coupling**

The amine (1.0 eq), carboxylic acid (1.0 – 1.2 eq), EDCI (1.2 eq) and HOBt (1.1 eq) were combined in an acetonitrile solution (10 mL/mmol amine) and stirred at rt for the specified time. The solvent was removed (not required for ≤ 5.0 mL acetonitrile) and the residue was dissolved in EtOAc (25 mL for reactions that contained ≤ 1.0 mmol amine or 25 mL/mmol amine for larger scale reactions). The organic solution was washed successively with aqueous HCl (1.0 M – 2 × 25 mL), saturated aqueous NaHCO<sub>3</sub> (3 × 25 mL) and brine (1 × 25 mL). The EtOAc solution was dried (MgSO<sub>4</sub>), filtered and concentrated. If necessary, the residue was subjected to further purification *via* flash chromatography over SiO<sub>2</sub> gel to furnish the targeted amide product.

##### **General Procedure C: Amine deprotection (*N*-Boc and/or *N*-Pbf removal)**

The *N*-protected amine (1.0 eq) was dissolved in a CH<sub>2</sub>Cl<sub>2</sub> (30 mL/mmol substrate) with magnetic stirring. If the substrate molecule contained an *N*-Pbf moiety then H<sub>2</sub>O (20.0 eq) was also added to the solution. TFA (30.0 mL/mmol substrate) was then added and the reaction mixture was stirred at rt overnight (> 16 h) followed by removal of the solvent. The residue was dissolved in CH<sub>2</sub>Cl<sub>2</sub> (30 mL/mmol substrate), an excess amount of anhydrous HCl (2.0 M in Et<sub>2</sub>O, 15 mL/mmol substrate, 30.0 eq) was added and the solvent was then removed. The resulting residue was dissolved in a minimal volume of CH<sub>2</sub>Cl<sub>2</sub> (or MeOH) and excess Et<sub>2</sub>O (25 mL for ≤ 0.1 mmol substrate) was added to precipitate the hydrochloride salt of the amine. The solvent was removed by filtration and the product (both in the filter funnel and in the flask) was triturated with Et<sub>2</sub>O (3 × 20 mL). The product was collected by dissolution in MeOH; concentration followed by drying *in vacuo* gave the final mono- or di-hydrochloride salt as a thin, translucent film that was routinely scratched with a spatula into a fine hygroscopic powder or amorphous gum.

##### **General Procedure D: Modified amine deprotection (*N*-Boc removal)**

For the biphenyl monocationic lysine derivatives (**38–40**), **General Procedure C** was followed with the following modifications: Et<sub>2</sub>O (instead of CH<sub>2</sub>Cl<sub>2</sub> or MeOH) was utilized to dissolve the residue for final precipitation and petroleum spirits (P.S. – instead of Et<sub>2</sub>O) was utilized as the antisolvent for precipitation.

### 4.3. Representative synthesis of compound **28** from precursor building blocks **12** and **15**

(*R*)-2-(4-(((2'-(Isopentyloxy)-[1,1'-biphenyl]-2-yl)oxy)methyl)-1*H*-1,2,3-triazol-1-yl)-5-(2-((2,2,4,6,7-pentamethyl-2,3-dihydrobenzofuran-5-yl)sulfonyl)guanidino)pentanoic acid (**17**)

Following **General Procedure A**, azide **15** (1.20 g, 2.65 mmol), alkyne **12** (1.56 g, 5.30 mmol), Cu(OAc)<sub>2</sub>·H<sub>2</sub>O (106 mg, 0.53 mmol) and sodium ascorbate (210 mg, 1.06 mmol) were stirred in *t*-BuOH (53 mL) and H<sub>2</sub>O (13.3 mL) for 18 h to give the product triazole **17** (1.63 g, 82%) as a translucent tan gum after flash chromatography over SiO<sub>2</sub> gel (EtOAc/P.S. – 10:90 → MeOH/CH<sub>2</sub>Cl<sub>2</sub> – 10:90). TLC (MeOH/CH<sub>2</sub>Cl<sub>2</sub> – 10:90): R<sub>f</sub> = 0.40, (EtOAc/P.S. – 80:20): R<sub>f</sub> = 0.42; [α]<sub>D</sub><sup>23</sup> –28.1 (*c* 1.03, MeOH); <sup>1</sup>H NMR (400 MHz, DMSO) δ 7.84 (s, 1H, H5'), 7.60 (br s, 1H), 7.33 – 7.18 (m, 3H), 7.18 – 7.10 (m, 2H), 7.01 – 6.94 (m, 2H), 6.88 (t, *J* = 7.3 Hz, 1H), 6.80 (br s, 2H), 5.06 (s, 2H), 4.91 (br s, 1H), 3.93 – 3.81 (m, 2H), 3.07 – 2.96 (m, 2H), 2.94 (s, 2H), 2.47 (s, 3H), 2.41 (s, 3H), 2.22 – 2.07 (m, 1H), 1.99 (s, 3H), 1.91 – 1.77 (m, 1H), 1.54 (td, *J* = 13.2, 6.6 Hz, 1H), 1.45 – 1.33 (m, 8H), 1.23 (br s, 1H), 1.07 (br s, 1H), 0.76 (d, *J* = 6.6 Hz, 6H); <sup>13</sup>C NMR (101 MHz, DMSO) δ 157.4, 156.32, 156.27, 156.1, 155.7, 142.6, 137.2, 134.3, 131.4, 131.2, 131.1, 128.5, 128.4, 127.9, 127.4, 124.3, 123.1, 120.4, 119.9, 116.2, 113.0, 112.2, 86.2, 66.2, 64.9, 62.2, 42.5, 39.5 (observed by gHSQC), 37.5, 30.2, 28.3, 25.9, 24.5, 22.4\*, 18.9, 17.6, 12.3; IR (neat) ν<sub>max</sub> 3327, 2946, 2873, 2831, 2363, 2167, 2027, 1617, 1559, 1506, 1442, 1405, 1238, 1108, 1023, 804, 751, 668 cm<sup>-1</sup>; MS (ESI +ve) *m/z* 747 ([M + H]<sup>+</sup>, 100%), MS (ESI –ve) *m/z* 745 ([M – H]<sup>-</sup>, 100%); HRMS (ESI +ve TOF) calcd for C<sub>39</sub>H<sub>51</sub>N<sub>6</sub>O<sub>7</sub>S 747.3540, found 747.3572 ([M + H]<sup>+</sup>).

(*R*)-*N*-Cyclohexyl-5-guanidino-2-(4-(((2'-(isopentyloxy)-[1,1'-biphenyl]-2-yl)oxy)methyl)-1*H*-1,2,3-triazol-1-yl)pentanamide hydrochloride (**28**)

Following **General Procedure B**, acid **17** (50 mg, 0.07 mmol), cyclohexylamine (8 mg, 0.08 mmol), EDCI (15 mg, 0.08 mmol) and HOBt (11 mg, 0.07 mmol) were stirred in acetonitrile (0.7 mL) for 21 h to give the intermediate amide as a translucent tan gum. Following **General Procedure C**, the amide was dissolved in CH<sub>2</sub>Cl<sub>2</sub> (2.0 mL) and treated with H<sub>2</sub>O (24 mg, 1.34 mmol) and CF<sub>3</sub>CO<sub>2</sub>H (2.0 mL) followed by work-up with ethereal HCl to give the amine salt **28** (39 mg, 95% over two steps) as a light tan powder that rapidly transitioned to a sticky gum. [α]<sub>D</sub><sup>23</sup> +15.9 (*c* 0.83, MeOH); <sup>1</sup>H NMR (400 MHz, CD<sub>3</sub>OD) δ 7.77 (s, 1H), 7.34 – 7.24 (m, 2H), 7.23 – 7.09 (m, 3H), 7.05 – 6.98 (m, 2H), 6.95 (t, *J* = 7.4 Hz, 1H), 5.24 (t, *J* = 7.7 Hz, 1H), 5.14 – 5.05 (m, 2H), 3.96 – 3.85 (m, 2H), 3.68 – 3.57 (m, 1H), 3.18 (t, *J* = 7.0 Hz, 2H), 2.22 – 2.00 (m, 2H), 1.92 – 1.12 (m, 15H), 0.77 (d, *J* = 6.6 Hz, 6H); <sup>13</sup>C NMR (101 MHz, CD<sub>3</sub>OD) δ 168.7, 158.8, 158.2, 157.5, 146.2, 132.7, 132.5, 130.7\*, 129.9, 129.7, 124.0, 122.5, 121.5, 114.7, 113.8, 68.2, 64.8, 64.1, 50.4, 41.9, 39.4, 33.7, 33.6, 31.1, 26.7, 26.4, 26.3, 26.20, 26.16, 23.1\*; IR (neat) ν<sub>max</sub> 3329, 3185, 3067, 2953, 2929, 2868, 2364, 2323, 1684, 1669, 1653, 1617, 1559, 1540, 1507, 1473, 1457, 1437, 1387, 1363, 1340, 1213, 1123, 1108, 1088, 1040, 1003, 941, 855, 802, 749, 668 cm<sup>-1</sup>; MS (ESI +ve) *m/z* 576 ([M + H]<sup>+</sup>, 100%), 598 ([M + Na]<sup>+</sup>, 19%); HRMS (ESI +ve TOF) calcd for C<sub>32</sub>H<sub>46</sub>N<sub>7</sub>O<sub>3</sub> 576.3662, found 576.3688 ([M + H]<sup>+</sup>).

### 4.4. Microbiology assays

#### 4.4.1. Primary screening (Gram-positive bacteria)

Primary MIC assays were performed as described by the Clinical and Laboratory Standards Institute for aerobic [49] and anaerobic [50] bacteria. *S. aureus* strains ATCC 29213 and NCTC 10442 (MRSA) and *E. faecalis* (ATCC 29212) were tested in Mueller Hinton broth (MHB) and incubation was performed in ambient air at 35 °C for 24 h. *S. pneumoniae* (ATCC 49619) was cultivated in MHB with 2.5% lysed horse blood and incubated with 5% CO<sub>2</sub> at 35 °C for 24 h. MIC studies for *C. difficile* strains ATCC 700057 and NSW132 (RT027) were conducted in pre-reduced (2-4 h) Brucella broth supplemented with haemin and vitamin K and incubation was performed anaerobically at 35 °C in a Don Whitley Scientific anaerobic chamber (A35) for 48 h. Each compound was dissolved in DMSO at 5 mg/mL and then diluted to 512 μg/mL with sterile, distilled water. The compounds were then serially diluted in 100 μL volumes of sterile, distilled water in a 96-well microtitre tray. Each test organism in double strength broth (100 μL) was then added to each well and incubated as described above. Final testing concentrations of the compounds ranged from 0.25 μg/mL to 128 μg/mL. Vancomycin and a control well

(i.e. no antibacterial compound present) were included in the assays. A DMSO control (5% v/v) was also tested to ensure that the solvent did not inhibit bacterial growth. The assay was performed in triplicate for each organism/compound combination and the modal MIC values were recorded. The MIC was determined visually as the lowest concentration that inhibited bacterial growth. Concentrations of  $\leq 5\%$  DMSO were not inhibitory to growth. MIC values for vancomycin were within acceptable QC ranges [51].

#### 4.4.2. Secondary screening (MRSA and Gram-negative bacteria) and cytotoxicity assay – performed by the Community for Open Antimicrobial Drug Discovery (CO-ADD)

Samples were provided to CO-ADD [34] for antimicrobial screening by whole cell growth inhibition assays. The inhibition of growth was measured against five bacteria: *E. coli* (ATCC 25922), *K. pneumoniae* (ATCC 700603), *A. baumannii* (ATCC 19606), *P. aeruginosa* (ATCC 27853) and *S. aureus* (ATCC 43300). In addition to the MIC assay, compounds were screened for cytotoxicity against a human embryonic kidney cell line (HEK293) by determining their  $CC_{50}$  value. Samples were prepared in DMSO to a final testing concentration of 32  $\mu\text{g/mL}$  and serially diluted 1:2 fold for 8 times. Each sample concentration was prepared in 384-well plates; non-binding surface (NBS) plates (Corning 3640) for each bacterial strain and black plates (Corning 3712/3764) for mammalian cell types, all in duplicate ( $n = 2$ ) and keeping the final DMSO concentration to a maximum of 0.5%. All the sample preparation was done using liquid handling robots.

##### *Bacterial Inhibition – MIC Assay*

All bacteria were cultured in Cation-adjusted MHB at 37 °C overnight. A sample of each culture was then diluted 40-fold in fresh broth and incubated at 37 °C for 1 – 3.5 h. The resultant mid-log phase cultures were diluted (CFU/mL measured by  $OD_{600}$ ), then added to each well of the compound-containing plates, giving a cell density of  $5 \times 10^5$  CFU/mL and a total volume of 50  $\mu\text{L}$ . All plates were covered and incubated at 37 °C for 18 h without shaking. Inhibition of bacterial growth was determined by measuring absorbance at 600 nm ( $OD_{600}$ ), using a Tecan M1000 Pro monochromator plate reader. The percentage of growth inhibition was calculated for each well, using the negative control (media only) and positive control (bacteria without inhibitors) on the same plate as references. The MIC was determined as the lowest concentration at which growth was fully inhibited, defined by an inhibition  $\geq 80\%$ . Colistin and vancomycin were used as positive bacterial inhibitor standards for Gram-negative and Gram-positive bacteria, respectively. Each antibiotic standard was provided in four concentrations, with two above and two below its MIC value, and plated into the first eight wells of column 23 of the 384-well NBS plates.

##### *Cytotoxicity Assay*

HEK293 cells were counted manually in a Neubauer haemocytometer and then plated in the 384-well plates containing the compounds to give a density of 5000 cells/well in a final volume of 50  $\mu\text{L}$ . Dulbecco's modified eagle medium (DMEM) supplemented with 10% fetal bovine serum (FBS) was used as a growth media and the cells were incubated together with the compounds for 20 h at 37 °C in 5%  $\text{CO}_2$ . Cytotoxicity (cell viability) was measured by fluorescence (ex: 560/10 nm, em: 590/10 nm), after addition of 5  $\mu\text{L}$  of 25  $\mu\text{g/mL}$  resazurin (2.3  $\mu\text{g/mL}$  final concentration) and after incubation for further 3 h at 37 °C in 5%  $\text{CO}_2$ . The fluorescence intensity was measured using a Tecan M1000 Pro monochromator plate reader, using automatic gain calculation.  $CC_{50}$  (concentration at 50% cytotoxicity) values were calculated by curve-fitting the inhibition values vs.  $\log(\text{concentration})$  using a sigmoidal dose-response function, with variable fitting values for bottom, top and slope. Tamoxifen was utilized as a positive cytotoxicity standard; it was used in eight concentrations in two-fold serial dilutions with 50  $\mu\text{g/mL}$  as the highest concentration tested.

#### 4.4.3. Haemolysis assay

The haemolytic activity of the synthesized compounds was determined by lysis of sheep erythrocytes. Briefly, 500  $\mu\text{L}$  volumes of each compound in phosphate buffer solution (PBS) were mixed with 480  $\mu\text{L}$  PBS and 20  $\mu\text{L}$  washed sheep erythrocytes (100%) in microcentrifuge tubes; this produced a final erythrocyte concentration of 2%. Compounds were tested at both 5  $\mu\text{g/mL}$  and 50  $\mu\text{g/mL}$ . A positive control (980  $\mu\text{L}$  water and 20  $\mu\text{L}$  erythrocytes) and a negative control (980  $\mu\text{L}$  PBS and 20  $\mu\text{L}$  erythrocytes) were also included in the assay. The centrifuge tubes were incubated on a rocker at 37 °C for 2 h and then centrifuged at 12,000 rpm for 5 min; 100  $\mu\text{L}$  volumes of the supernatant fluid were transferred to a 96-well microtitre tray and the optical density of the samples was observed at 540 nm. The value for the negative control was subtracted from the haemolysis values



and then the resulting quantities were expressed as a percentage of the positive control (which was defined as 100% haemolysis). The haemolysis assay was repeated in triplicate for all compounds and the mean values were reported.

#### 4.4.4. Cytoplasmic membrane depolarization assay

An inoculum containing 1.5 McFarland standard of mid-log cells (*S. aureus* ATCC 29213 or *E. coli* NCTC 10418) was suspended in either phosphate buffered saline (PBS – for *S. aureus*) or a 5 mM HEPES solution containing 20 mM glucose adjusted to pH 7.2 (for *E. coli*). Then, 3,3'-dipropylthiadicarbocyanine (diSC<sub>3</sub>(5)) was added at 4 µM to the bacteria suspension and the mixture was incubated in the dark at room temperature (30 min for *S. aureus* and 60 min for *E. coli*). For *E. coli* only, KCl was then added at 100 mM, followed by EDTA at 0.5 mM. Then, 100 µL aliquots of the bacterial suspension were added to wells of a 96-well plate (black with clear bottom); the fluorescence was tracked (ex: 620/10 nm, em: 670/10 nm) for approximately 8 min prior to exposure to the test compounds. The content of each well was then transferred to a different well containing 100 µL of one of the various test compounds prepared at double the final test concentration. The fluorescence was then tracked for approximately 30 min. The final assay concentration of the test compounds was 32 µg/mL for *S. aureus* and 64 µg/mL for *E. coli*. UltraPure H<sub>2</sub>O was utilized as a negative control for both species. DMSO (20%) was utilized as a positive control for both species. Vancomycin (8 µg/mL) was used as a negative control for *S. aureus* and colistin (64 µg/mL) was used as positive control for *E. coli*.

#### 4.4.5. Cytoplasmic membrane permeabilization assay

An inoculum containing 1.5 McFarland standard of mid-log cells (*S. aureus* ATCC 29213 or *E. coli* NCTC 10418) was suspended in either phosphate buffered saline (PBS – for *S. aureus*) or a 5 mM HEPES solution containing 20 mM glucose adjusted to pH 7.2 (for *E. coli*). Then, propidium iodide was added at 4 µM to the bacteria suspension and the mixture was incubated in the dark at room temperature (30 min for *S. aureus* and 60 min for *E. coli*). For *E. coli* only, KCl was then added at 100 mM, followed by EDTA at 0.5 mM. Then, 100 µL aliquots of the bacterial suspension were added to wells of a 96-well plate (black with clear bottom); the fluorescence was tracked (ex: 544/10 nm, em: 615/10 nm) for approximately 8 min prior to exposure to the test compounds. The content of each well was then transferred to a different well containing 100 µL of one of the various test compounds prepared at double the final test concentration. The fluorescence was then tracked for approximately 30 min. The final assay concentration of the test compounds was 32 µg/mL for both *S. aureus* and *E. coli*. UltraPure H<sub>2</sub>O was utilized as a negative control for both species. Vancomycin (8 µg/mL) was used as a negative control for *S. aureus* and colistin (64 µg/mL) was used as a positive control for *E. coli*.

### 4.5. In vivo murine model of CDI treatment

#### 4.5.1. Disease treatment model

*C. difficile* spores from strain M7404 [46] were prepared for mouse infection experiments as previously described [45]. Animal handling and experimentation was performed in accordance with Victorian State Government regulations and approved by the Monash University Animal Ethics Committee (Monash University AEC no. MARP/2014/142). Groups of male, C57BL/6J, six week old mice (Walter and Eliza Hall Institute of Medical Research, Melbourne, Australia) were pre-treated with an antibiotic cocktail to induce susceptibility to infection as previously described [52]. Mice were administered 10<sup>5</sup> *C. difficile* spores by oral gavage. Six hours post-infection and then every 12 hours thereafter, mice were administered 2.5 mg (100 mg/kg in 10% DMSO) of the test compound, 10% DMSO or vancomycin (100 µL of a 4 mg/mL solution) by oral gavage. Mice were monitored daily for signs of disease (weight loss, diarrhoea, behavioural and physiological changes). Feces were collected 1 day post-infection to enumerate *C. difficile* spore load. Fecal pellets were resuspended in PBS (100 mg/ml), heat shocked (30 minutes, 65 °C) and plated for spore enumeration as described previously [52]. Disease severity was assessed at 1 day post-infection by scoring the overall cage appearance (Table S1) as well as individual mouse fecal consistency (Table S2) and physiological appearance (Table S3). Mice were humanely killed at the onset of severe disease or at the end of the experiment (day 4), as previously defined [53].

#### 4.5.2. Statistical analysis

Statistical analysis was performed using Prism 7 (GraphPad Software). The Kaplan-Meier survival curves were assessed using a log-rank (Mantel-Cox) test. Weight loss, spore shedding, fecal consistency and physiological appearance data were analysed by one-way ANOVA with a *post-hoc Tukeys* multiple comparison test. Differences in data values were considered significant at a *P* value of < .05.

#### 4.6. Pharmacokinetics assay

##### 4.6.1. Mouse blood analysis

A 200  $\mu$ L aliquot of the mouse blood was placed into a glass vial and diluted with phosphate buffered saline (PBS) solution (3.3 mL). The solution was vortexed for 20 s and then  $\text{CH}_2\text{Cl}_2$  (3.5 mL) was added and the mixture was manually swirled to ensure adequate mixing with minimal emulsion formation. The layers were allowed to separate and the  $\text{CH}_2\text{Cl}_2$  was removed by syringe. The aqueous blood layer was extracted again with another aliquot of  $\text{CH}_2\text{Cl}_2$  (3.5 mL). The two extracts were combined and evaporated under reduced pressure to obtain an opaque residue. The residue was dissolved in MeOH (2.0 mL) with the aid of ultrasonication (30 s); the solution was filtered through a PTFE membrane filter (0.45  $\mu$ m). The obtained solution was then subjected to LRMS analysis.

##### 4.6.2. Mouse blood analysis: procedure verification

To ensure the mouse blood analysis procedure was sufficiently sensitive to detect small amounts of drug absorption, unadulterated mouse blood (i.e. blood from an untreated cohort) was doped with compound **67** and then subjected to the analysis procedure. The volume of mouse blood was accounted for to ensure that an accurate concentration representative of a 1% systemic bioavailability was achieved. To dope the blood with the correct concentration, 50  $\mu$ L of a 0.05 mg/mL solution of compound **67** in 0.1% DMSO in  $\text{H}_2\text{O}$  was added to the PBS diluent prior to completion of the analysis procedure. The blood/PBS/compound mixture was also allowed to rest for 2 h prior to extraction with  $\text{CH}_2\text{Cl}_2$  and completion of the analysis procedure (Section 4.6.1.).

##### 4.6.3. Mouse feces analysis

The obtained sample of mouse feces (from the cohort treated with compound **67**) was added to a glass vial with  $\text{CH}_2\text{Cl}_2$  (2.0 mL) and the mixture was stirred vigorously for 30 min. The solution was then filtered through a cotton plug and the solvent was removed under reduced pressure. The residue was taken up in MeOH (1.0 mL), sonicated for 30 s and then filtered through a PTFE membrane filter (0.45  $\mu$ m). The obtained solution was then subjected to LRMS analysis.

#### Acknowledgements

The authors thank the Australian National Health and Medical Research Council (NHMRC) for financial support (Grant #APP1124032). The authors also thank Meagan James and Chris Evans for assistance with mouse infection experiments.

#### Appendix A. Supplementary information

Supplementary information related to this article can be found at <https://doi.org/10.1016/j.ejmech.2019.02.068>.

## References

1. Leffler, D. A.; Lamont, J. T. Treatment of *Clostridium difficile*-Associated Disease. *Gastroenterology* **2009**, *136* (6), 1899-1912.
2. Eaton, S. R.; Mazuski, J. E. Overview of Severe *Clostridium difficile* Infection. *Crit. Care Clin.* **2013**, *29* (4), 827.
3. Jarrad, A. M.; Karoli, T.; Blaskovich, M. A. T.; Lyras, D.; Cooper, M. A. *Clostridium difficile* Drug Pipeline: Challenges in Discovery and Development of New Agents. *J. Med. Chem.* **2015**, *58* (13), 5164-5185.
4. Johnson, A. P. New antibiotics for selective treatment of gastrointestinal infection caused by *Clostridium difficile*. *Expert Opin. Ther. Patents* **2010**, *20* (10), 1389-1399.
5. Centers for Disease Control and Prevention. *Clostridium difficile* Update. **2015**. <https://www.cdc.gov/media/releases/2015/p0225-clostridium-difficile.html> (accessed June 12th, 2018).
6. Centers for Disease Control and Prevention. Antibiotic Resistance Threats in the United States. **2013**. <https://www.cdc.gov/drugresistance/threat-report-2013/index.html> (accessed June 12th, 2018).
7. Stanley, J. D.; Bartlett, J. G.; Dart, B. W.; Ashcraft, J. *Clostridium difficile* infection. *Curr. Probl. Surg.* **2013**, *50* (7), 302-337.
8. Ritter, A. S.; Petri, W. A. New developments in chemotherapeutic options for *Clostridium difficile* colitis. *Curr. Opin. Infect. Dis.* **2013**, *26* (5), 461-470.
9. Cornely, O. A.; Miller, M. A.; Louie, T. J.; Crook, D. W.; Gorbach, S. L. Treatment of First Recurrence of *Clostridium difficile* Infection: Fidaxomicin Versus Vancomycin. *Clin. Infect. Dis.* **2012**, *55*, S154-S161.
10. Hostler, C. J.; Chen, L. F. Fidaxomicin for treatment of *Clostridium difficile*-associated diarrhea and its potential role for prophylaxis. *Expert Opin. Pharmacother.* **2013**, *14* (11), 1529-1536.
11. Critchley, I. A.; Green, L. S.; Young, C. L.; Bullard, J. M.; Evans, R. J.; Price, M.; Jarvis, T. C.; Guiles, J. W.; Janjic, N.; Ochsner, U. A. Spectrum of activity and mode of action of REP3123, a new antibiotic to treat *Clostridium difficile* infections. *J. Antimicrob. Chemother.* **2009**, *63* (5), 954-963.
12. Nayak, S. U.; Griffiss, J. M.; Blumer, J.; O'Riordan, M. A.; Gray, W.; McKenzie, R.; Jurao, R. A.; An, A. T.; Le, M.; Bell, S. J.; Ochsner, U. A.; Jarvis, T. C.; Janjic, N.; Zenilman, J. M. Safety, tolerability, systemic exposure and metabolism of CRS3123, a methionyl-tRNA synthetase inhibitor developed for treatment of *Clostridium difficile* infections, in a Phase I study. *Antimicrob. Agents Chemother.* **2017**, *61* (8): e02760-16.
13. LaMarche, M. J.; Leeds, J. A.; Amaral, A.; Brewer, J. T.; Bushell, S. M.; Deng, G.; Dewhurst, J. M.; Ding, J.; Dzink-Fox, J.; Zhu, Q.; *et al.* Discovery of LFF571: An Investigational Agent for *Clostridium difficile* Infection. *J. Med. Chem.* **2012**, *55* (5), 2376-2387.
14. Trzasko, A.; Leeds, J. A.; Praestgaard, J.; LaMarche, M. J.; McKenney, D. Efficacy of LFF571 in a Hamster Model of *Clostridium difficile* Infection. *Antimicrob. Agents Chemother.* **2012**, *56* (8), 4459-4462.
15. Leeds, J. A.; Sachdeva, M.; Mullin, S.; Dzink-Fox, J.; LaMarche, M. J. Mechanism of action of, and mechanism of reduced susceptibility to the novel anti-*Clostridium difficile* compound LFF571. *Antimicrob. Agents Chemother.* **2012**, *56* (8), 4463-4465.
16. Mullane, K.; Lee, C.; Bressler, A.; Buitrago, M.; Weiss, K.; Dabovic, K.; Praestgaard, J.; Leeds, J. A.; Blais, J.; Pertel, P. Multicenter, Randomized Clinical Trial To Compare the Safety and Efficacy of LFF571

- and Vancomycin for *Clostridium difficile* Infections. *Antimicrob. Agents Chemother.* **2015**, *59* (3), 1435-1440.
17. Crowther, G. S.; Baines, S. D.; Todhunter, S. L.; Freeman, J.; Chilton, C. H.; Wilcox, M. H. Evaluation of NVB302 versus vancomycin activity in an in vitro human gut model of *Clostridium difficile* infection. *J. Antimicrob. Chemother.* **2013**, *68* (1), 168-176.
  18. Mann, J.; Taylor, P. W.; Dorgan, C. R.; Johnson, P. D.; Wilson, F. X.; Vickers, R.; Dale, A. G.; Neidle, S. The discovery of a novel antibiotic for the treatment of *Clostridium difficile* infections: a story of an effective academic–industrial partnership. *MedChemComm* **2015**, *6* (8), 1420-1426.
  19. Vickers, R. J.; Tillotson, G.; Goldstein, E. J. C.; Citron, D. M.; Garey, K. W.; Wilcox, M. H. Ridinilazole: a novel therapy for *Clostridium difficile* infection. *Int. J. Antimicrob. Agents* **2016**, *48* (2), 137-143.
  20. Endres, B. T.; Bassères, E.; Alam, M. J.; Garey, K. W. Cadazolid for the treatment of *Clostridium difficile*. *Expert Opin. Investig. Drugs* **2017**, *26* (4), 509-514.
  21. Kali, A.; Charles, M. V. P.; Srirangaraj, S. Cadazolid: A new hope in the treatment of *Clostridium difficile* infection. *Australas. Med. J.* **2015**, *8* (8), 253-262.
  22. Actelion, Ltd. Phase III Clinical Trial Results (News Conference). <https://www1.actelion.com/en-rebranded/investors/news-archive.page?newsId=2111437> (accessed 12/07/2018).
  23. Dvoskin, S.; Xu, W.-C.; Brown, N. C.; Yanachkov, I. B.; Yanachkova, M.; Wright, G. E. A Novel Agent Effective against *Clostridium difficile* Infection. *Antimicrob. Agents Chemother.* **2012**, *56* (3), 1624-1626.
  24. Kirst, H. A.; Toth, J. E.; Debono, M.; Willard, K. E.; Truedell, B. A.; Ott, J. L.; Counter, F. T.; Felty-Duckworth, A. M.; Pekarek, R. S. Synthesis and evaluation of tylosin-related macrolides modified at the aldehyde function: a new series of orally effective antibiotics. *J. Med. Chem.* **1988**, *31* (8), 1631-1641.
  25. Ballard, T. E.; Wang, X.; Olekhnovich, I.; Koerner, T.; Seymour, C.; Hoffman, P. S.; Macdonald, T. L. Biological Activity of Modified and Exchanged 2-Amino-5-Nitrothiazole Amide Analogues of Nitazoxanide. *Bioorg. Med. Chem. Lett.* **2010**, *20* (12), 3537-3539.
  26. Zhang, S.J.; Yang, Q.; Xu, L.; Chang, J.; Sun, X. Synthesis and antibacterial activity against *Clostridium difficile* of novel demethylvancomycin derivatives. *Bioorg. Med. Chem. Lett.* **2012**, *22* (15), 4942-4945.
  27. Ueda, C.; Tateda, K.; Horikawa, M.; Kimura, S.; Ishii, Y.; Nomura, K.; Yamada, K.; Suematsu, T.; Inoue, Y.; Ishiguro, M.; Miyairi, S.; Yamaguchi, K. Anti-*Clostridium difficile* Potential of Tetramic Acid Derivatives from *Pseudomonas aeruginosa* Quorum-Sensing Autoinducers. *Antimicrob. Agents Chemother.* **2010**, *54* (2), 683-688.
  28. Tague, A. J.; Putsathit, P.; Hammer, K. A.; Wales, S. M.; Knight, D.R.; Riley, T. V.; Keller, P. A.; Pyne, S.G. Cationic biaryl 1,2,3-triazolyl peptidomimetic amphiphiles: synthesis and antibacterial evaluation. **Submitted Manuscript - European Journal of Medicinal Chemistry, 2018.**
  29. Wales, S. M.; Hammer, K. A.; King, A. M.; Tague, A. J.; Lyras, D.; Riley, T. V.; Keller, P. A.; Pyne, S. G. Binaphthyl-1,2,3-triazole peptidomimetics with activity against *Clostridium difficile* and other pathogenic bacteria. *Org. Biomol. Chem.* **2015**, *13* (20), 5743-5756.
  30. Liu, R.; Suárez, J. M.; Weisblum, B.; Gellman, S. H.; McBride, S. M. Synthetic Polymers Active against *Clostridium difficile* Vegetative Cell Growth and Spore Outgrowth. *J. Am. Chem. Soc.* **2014**, *136* (41), 14498-14504.

31. Butler, M. M.; Williams, J. D.; Peet, N. P.; Moir, D. T.; Panchal, R. G.; Bavari, S.; Shinabarger, D. L.; Bowlin, T. L. Comparative *In Vitro* Activity Profiles of Novel Bis-Indole Antibacterials against Gram-Positive and Gram-Negative Clinical Isolates. *Antimicrob. Agents Chemother.* **2010**, *54* (9), 3974-3977.
32. Lowes, R. FDA Approves Zinplava for Preventing Return of *C. difficile*. <https://www.medscape.com/viewarticle/870887> (accessed June 12<sup>th</sup>, 2018).
33. Bremner, J. B.; Keller, P. A.; Pyne, S. G.; Boyle, T. P.; Brkic, Z.; David, D. M.; Garas, A.; Morgan, J.; Robertson, M.; Somphol, K.; *et al.* Binaphthyl-Based Dicationic Peptoids with Therapeutic Potential. *Angew. Chem.-Int. Edit.* **2010**, *49* (3), 537-540.
34. Bremner, J. B.; Keller, P. A.; Pyne, S. G.; Boyle, T. P.; Brkic, Z.; David, D. M.; Robertson, M.; Somphol, K.; Baylis, D.; Coates, J. A.; *et al.* Synthesis and antibacterial studies of binaphthyl-based tripeptoids. Part 1. *Bioorg. Med. Chem.* **2010**, *18* (7), 2611-2620.
35. Bremner, J. B.; Keller, P. A.; Pyne, S. G.; Boyle, T. P.; Brkic, Z.; Morgan, J.; Somphol, K.; Coates, J. A.; Deadman, J.; Rhodes, D. I. Synthesis and antibacterial studies of binaphthyl-based tripeptoids. Part 2. *Bioorg. Med. Chem.* **2010**, *18* (13), 4793-4800.
36. Ghosh, C.; Manjunath, G. B.; Akkapeddi, P.; Yarlagadda, V.; Hoque, J.; Uppu, D.; Konai, M. M.; Haldar, J. Small Molecular Antibacterial Peptoid Mimics: The Simpler the Better! *J. Med. Chem.* **2014**, *57* (4), 1428-1436.
37. Kuppusamy, R.; Yasir, M.; Berry, T.; Cranfield, C. G.; Nizalapur, S.; Yee, E.; Kimyon, O.; Taunk, A.; Ho, K. K. K.; Cornell, B.; Manefield, M.; Willcox, M.; Black, D. S.; Kumar, N. Design and synthesis of short amphiphilic cationic peptidomimetics based on biphenyl backbone as antibacterial agents. *Eur. J. Med. Chem.* **2018**, *143*, 1702-1722.
38. Wales, S. M.; Hammer, K. A.; Somphol, K.; Kemker, I.; Schroder, D. C.; Tague, A. J.; Brkic, Z.; King, A. M.; Lyras, D.; Riley, T. V.; Bremner, J. B.; Keller, P. A.; Pyne, S. G. Synthesis and antimicrobial activity of binaphthyl-based, functionalized oxazole and thiazole peptidomimetics. *Org. Biomol. Chem.* **2015**, *13* (44), 10813-10824.
39. Garas, A.; Bremner, J. B.; Coates, J.; Deadman, J.; Keller, P. A.; Pyne, S. G.; Rhodes, D. I. Binaphthyl scaffolded peptoids via ring-closing metathesis reactions and their anti-bacterial activities. *Bioorg. Med. Chem. Lett.* **2009**, *19* (11), 3010-3013.
40. Khara, J. S.; Priestman, M.; Uhía, I.; Hamilton, M. S.; Krishnan, N.; Wang, Y.; Yang, Y. Y.; Langford, P. R.; Newton, S. M.; Robertson, B. D.; Ee, P. L. R. Unnatural amino acid analogues of membrane-active helical peptides with anti-mycobacterial activity and improved stability. *J. Antimicrob. Chemother.* **2016**, *71* (8), 2181-2191.
41. Sorg, G. Progress in the preparation of peptide aldehydes via polymer supported IBX oxidation and scavenging by threonyl resin. *J. Pept. Sci.* **11** (3), 142-152.
42. Rodriguez, M.; Llinares, M.; Doulut, S.; Heitz, A.; Martinez, J. A facile synthesis of chiral *N*-protected  $\beta$ -amino alcohols. *Tetrahedron Lett.* **1991**, *32* (7), 923-926.
43. Chen, C. C.; Rajagopal, B.; Liu, X. Y.; Chen, K. L.; Tyan, Y. C.; Lin, F.; Lin, P. C. A mild removal of Fmoc group using sodium azide. *Amino Acids* **2014**, *46* (2), 367-374.
44. Blaskovich, M. A. T.; Zuegg, J.; Elliott, A. G.; Cooper, M. A. Helping Chemists Discover New Antibiotics. *ACS Infect. Dis.* **2015**, *1* (7), 285-287.

45. Hutton, M. L.; Cunningham, B. A.; Mackin, K. E.; Lyon, S. A.; James, M. L.; Rood, J. I.; Lyras, D. Bovine antibodies targeting primary and recurrent *Clostridium difficile* disease are a potent antibiotic alternative. *Sci. Rep.* **2017**, *7*, 3665.
46. Carter, G. P.; Lyras, D.; Allen, D. L.; Mackin, K. E.; Howarth, P. M.; O'Connor, J. R.; Rood, J. I. Binary Toxin Production in *Clostridium difficile* Is Regulated by CdtR, a LytTR Family Response Regulator. *J. Bacteriol.* **2007**, *189* (20), 7290-7301.
47. Chu, W.-C.; Bai, P.-Y.; Yang, Z.-Q.; Cui, D.-Y.; Hua, Y.-G.; Yang, Y.; Yang, Q.-Q.; Zhang, E.; Qin, S. Synthesis and antibacterial evaluation of novel cationic chalcone derivatives possessing broad spectrum antibacterial activity. *Eur. J. Med. Chem.* **2018**, *143*, 905-921.
48. Zhang, E.; Bai, P.-Y.; Cui, D.-Y.; Chu, W.-C.; Hua, Y.-G.; Liu, Q.; Yin, H.-Y.; Zhang, Y.-J.; Qin, S.; Liu, H.-M. Synthesis and bioactivities study of new antibacterial peptide mimics: The dialkyl cationic amphiphiles. *Eur. J. Med. Chem.* **2018**, *143*, 1489-1509.
49. Clinical and Laboratory Standards Institute. Methods for Dilution Antimicrobial Susceptibility Tests for Bacteria That Grow Aerobically; Approved Standard – Ninth Edition. **2015**. CLSI Document M07-A10. *Clinical and Laboratory Standards Institute*, Wayne, Pennsylvania.
50. Clinical and Laboratory Standards Institute. Methods for Antimicrobial Susceptibility Testing of Anaerobic Bacteria; Approved Standard – Eighth Edition. **2012**. CLSI Document M11-A8. *Clinical and Laboratory Standards Institute*, Wayne, Pennsylvania.
51. Clinical Laboratory Standards Institute. Performance Standards for Antimicrobial Susceptibility Testing, 28th Informational Supplement. **2018**. CLSI document M100-S28. *Clinical and Laboratory Standards Institute*, Wayne, Pennsylvania.
52. Lyon, S. A.; Hutton, M. L.; Rood, J. I.; Cheung, J. K.; Lyras, D. CdtR Regulates TcdA and TcdB Production in *Clostridium difficile*. *PLoS Pathog.* **2016**, *12* (7), e1005758.
53. Carter, G. P.; Chakravorty, A.; Pham Nguyen, T. A.; Mileto, S.; Schreiber, F.; Li, L.; Howarth, P.; Clare, S.; Cunningham, B.; Sambol, S. P.; Lyras, D.; *et al.* Defining the Roles of TcdA and TcdB in Localized Gastrointestinal Disease, Systemic Organ Damage, and the Host Response during *Clostridium difficile* Infections. *mBio* **2015**, *6* (3), e00551-15.